1790A

DSC-5478-1

ORF

Final Report

for

RESEARCH ON A PASSIVE MODULATION INDUCING RETRODIRECTIVE OPTICAL SYSTEM (MIROS)

(20 May 1963 to 20 June 1964)

GPO PRICE $ _____

CFSTI PRICE(S) $ _____

Hard copy (HC) 3.00

Microfiche (MF) .75

ff 653 July 65

Contract No. NASw-703

Prepared by

WESTINGHOUSE DEFENSE AND SPACE CENTER
Aerospace Division
Baltimore, Maryland

for

GODDARD SPACE FLIGHT CENTER
Greenbelt, Maryland

FOREWORD

This report was prepared by the Westinghouse Defense and Space Center, Aerospace Division, Baltimore, Maryland, under National Aeronautics and Space Administration Contract No. NASw-703. It covers the theoretical and experimental effort conducted during a 12-month program to determine phenomena and techniques applicable to completely passive intelligence transfer by means of a retrodirective optical system.

Administration of the program by the monitoring agency was initially under Mr. R. H. Chase, Headquarters, Communication and Tracking Division, and was later transferred under the cognizance of Dr. H. Plotkin, Goddard Space Flight Center.

The program was conducted at Westinghouse Aerospace Division under the technical direction of Mr. J. B. Goodell, Fellow Engineer, Optical Maser Systems, Mr. C. R. Kline, Manager.

Chief contributors to the program were:

R. C. Gallagher
C. R. Kline
Dr. D. Mergerian
J. H. Lehman
Dr. K. Reinitz
E. Simonsen

J. B. Goodell

ABSTRACT

27527

This report represents the result of a year-long research program whose primary purpose was to investigate methods whereby one beam of light could be used to modulate another beam of light with no power other than that contained in the two beams supplied to the modulation transfer element. After 3 months spent in a preliminary investigation of all possible physical phenomena which might be useful in a passive modulation transfer device, it was concluded that the most promising modulation transfer schemes could be obtained by optical pumping methods. In these methods, absorption of light by the element creates a population inversion which results in a metastable energy level population increase. If light of frequency corresponding to transitions from this metastable level is incident on the element, because of the high population of the metastable energy level, the light will be absorbed.

Several possible optical pumping methods were investigated, and finally two materials were singled out for laboratory experimentation. One material was mercury vapor, the other was an alkali halide, potassium iodide. In the case of mercury vapor, the absorption-inducing line is the mercury 2537 Å resonance line, which corresponds to ground to first excited state transitions. The metastable 6^3P_0 level is populated by nitrogen quenching collisions. By populating this level, absorption of the 4047 Å line as high as 58 percent was observed. This modulation transfer scheme responded to modulation frequencies at least as high as 10 kc, where system noise made higher frequency measurements unreliable. Theoretical work was found to agree reasonably well with experiment. In the alkali halide experiment, the modulating line was in the infrared and the modulated line was at 6943 Å. Although complete experimental verification of this approach was not possible during the course of this program, results have been attained that show cross modulation is possible; however, frequency response is poor.

General formulas are derived which give an estimate of the powers necessary to induce absorption as well as to define the general aspects of the problem. An ideal power limit is estimated which represents modulation transfer capabilities using optical pumping.

TABLE OF CONTENTS

1. INTRODUCTION

2. PASSIVE MODULATION TRANSFER USING OPTICAL PUMPING METHODS

3. PASSIVE LIGHT MODULATION USING ALKALI HALIDES

4. MERCURY CELL EXPERIMENT

LIST OF ILLUSTRATIONS

LIST OF TABLES

1. INTRODUCTION

The Modulation-Inducing Retrodirective Optical System (MIROS) program was conceived primarily to determine the possibility of modulating one beam of light by another beam of light using no more power than is contained in the light beams. If this could be accomplished, passive communication transfer between the two optical beams would be achieved. Ultimately a retrodirective element such as a corner cube reflector, which contains a passive modulation transfer element, would be inserted in the path of two light beams, causing one beam to modulate the other beam - each beam returning to its source. Such an element could be installed in a satellite, where it would be used as a passive communication relay device between two widely separated points. In this case, the point desiring to transmit information would send a beam of light up to the passive modulation transfer element in the satellite. Because of the retrodirective properties of this system, this beam would return to the transmitter. From some other location, a receiving station would illuminate the retrodirective element. After being modulated by the transmitting beam, this illuminating beam would return to the receiver. Thus, passive information transfer from transmitter to receiver could be accomplished. Figure 1 is a schematic diagram of a MIROS system.

The advantages of such a passive modulation transfer device are obvious: long (possibly indefinite) operating life, elimination of need for local power supplies, and simplicity and flexibility usually unattainable where energy sources are necessary. All this, of course, presupposes that an efficient retrodirective modulation transfer element can be developed. The main advantage of a retrodirective element is wide angle coverage with a greater optical gain, as contrasted with an ordinary wide-angle communication system.

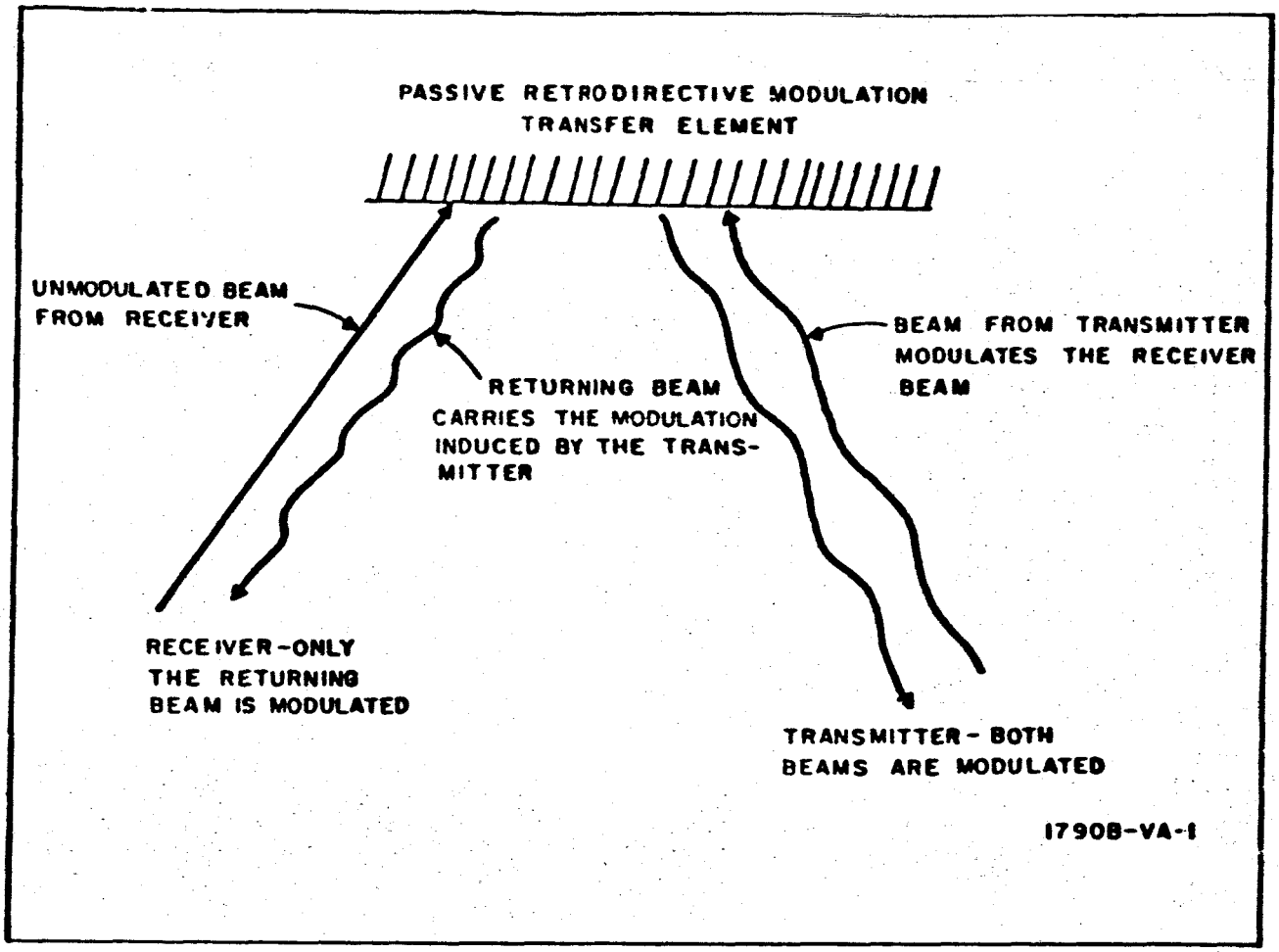

Figure 1. Schematic Diagram Illustrating a Modulation Inducing Retrodirective Optical Communication System

The most difficult part of the system from a developmental point of view is the passive modulation transfer element. This must consume no power other than that contained in the two incident light beams and must be capable of modulating the receiving beam a detectable amount and handling at least moderate communication rates. Translating these requirements into order of magnitude numbers, an ideal retrodirective element must consume at most no more than milliwatts of power and achieve, hopefully a few percent modulation at kilocycle bandwidths. This milliwatt figure is a maximum tolerable power; the more realistic operating power would fall in the microwatt region. These are severe requirements.

Because of the unusual requirements in this case, the usual research program approach was modified considerably. Many possible solutions were at first considered, almost without regard to physical realizability. Later the list was narrowed to a few promising techniques. Finally an experimental program was set up for two related modulation transfer schemes based on optical pumping methods which will be described in detail in this report. These two schemes operate on the physical principle that absorption by a material of light of one wavelength under certain conditions can cause absorption of light of another wavelength. The mechanism of this process is that absorption at one wavelength raises atoms in a material to a higher energy level, from which, by some process, they are induced to populate a metastable (long-lived) energy level. An increase in metastable population results in an increase in absorption coefficients corresponding to optical transitions from this level. Hence, if the receiver wavelength corresponds to one of these transitions, induced absoption of the receiver beam will occur upon irradiation of the material by the transmitter. The receiver beam will be amplitude modulated.

Pursuing a modulation scheme of this type obviously necessitates a research program to find materials which satisfy specific requirements. They are: (1) absorption at wavelengths corresponding to the transmitter beam must be strong; (2) the material must contain an energy level which can be easily populated; (3) a mechanism must exist for populating this level from the states excited by the transmitter beam; (4) transitions from this level, corresponding to receiver wavelengths, must have large absorption coefficients.

A surprising number of materials satisfy these requirements, at least to some degree. Quite often they also offer the mixed blessing of having narrow spectral responses. In one sense this is highly desirable because of background signal-to-noise consideration. In another sense this is not desirable since adequate light sources may not be available in the spectral regions in which they operate and their narrow spectral response permits almost no flexibility.

In this report, two materials capable of transferring optical modulation have been considered in detail. One is mercury vapor and the other is potassium iodide. In the mercury vapor modulation transfer element the transmitter light is at 2537 Å while the receiver light is at 4047 Å. In the potassium iodide element the transmitter light falls in either the near-infrared or red spectral region while the receiver light is either in the red or near-infrared region. The mechanisms by which metastable energy levels are populated in these two systems are similar in concept but differ considerably in detail.

2. PASSIVE MODULATION TRANSFER USING OPTICAL PUMPING METHODS

2.1 GENERAL

In the two passive modulation transfer schemes discussed in this report, two different mechanisms for populating metastables are employed. In the mercury vapor cell, ^3P_o metastable energy levels are populated when excited mercury atoms collide with nitrogen molecules. Thus, the mechanisms for producing high numbers of metastable atoms are resonance absorption followed by collisions of the second kind. On the other hand, in potassium iodide crystals a certain amount of energy is required to raise the excited F or F' center electron to the crystal conduction band from which it is captured by an F-center or negative ion vacancy. The mechanism in this case is therefore either F or F' absorption followed by phonon interaction.

Many mechanisms are available for populating metastable energy levels. Recent activity in the laser field has revealed many ingenious optical pumping techniques which no doubt might be extrapolated to passive modulation transfer devices, since there is a close connection between optical pumping as applied to lasers and optical pumping as applied to passive modulation transfer.

Associated with these techniques and pertinent materials are, of course, parameters such as spectral widths, pumping rates, and necessary powers, which can differ radically with different methods and materials. Solutions must naturally be worked out for each individual case to determine the feasibility of any particular method. Nevertheless, some general observations can be made which can give at least some insight into the phenomenon of passive modulation transfer by means of optical pumping techniques. This is the purpose of this section.

2.2 ESTIMATE OF MINIMUM POWER

Although each method of producing metastable energy level population requires a separate analysis and will have its own time constants, modulation depths, etc., an estimate of the minimum power required to produce a given modulation can be derived. This represents an upper limit for any passive modulation transfer scheme which uses the method of optical pumping.

Consider a volume of material of length d in which absorption of one beam is induced by incidence of another beam. In order to induce absorption of the receiver beam, photons must be absorbed from the transmitter beam. Suppose that each absorbed photon produces η electrons in the metastable level, uniformly distributed throughout the volume of the absorbing element. Then the intensity of the receiver beam after passing through the element can be written as

$$I_R = I_o e^{-\sigma n d} \qquad (1)$$

where:

σ = cross section for absorption

I_o = incident intensity of the receiver beam

n = number of absorbing centers which have appeared due to photon absorption of the transmitting beam.

This number is equal to:

$$\frac{\eta \lambda P \Delta t}{chabd} \qquad (2)$$

where:

P = power in the transmitter beam

t = a small time interval

h = Planck's constant

λ = wavelength of the transmitter radiation

c = velocity of light

a, b, d = dimensions of the element

If the modulation is defined by

$$M = \frac{I_o - I_R}{I_o} = 1 - e^{-\frac{\sigma \eta \lambda P \Delta t}{chab}} \qquad (3)$$

the power required to produce a given modulation of the receiver beam is

$$P = \frac{chab}{\sigma \eta \lambda \Delta t} \ln \left(\frac{1}{1-M}\right) \qquad (4)$$

This expression can hardly be called realistic, but it does give an estimate of the upper limit of the passive modulation transfer capabilities of any induced absorption process. A numerical estimate of the required power can be obtained by setting

$\sigma = 10^{-13}\ cm^2$

$\eta = 1$

$\lambda = 7000\ \mathring{A} = 7 \times 10^{-5}\ cm$

$ab = 1\ cm^2$

$h = 6.62 \times 10^{-34}$ joules - sec

$c = 3 \times 10^{10}$ cm/sec

Then the relation between P, t, and M becomes

$$P = \frac{2.8 \times 10^{-6}}{\Delta t} \ln \left(\frac{1}{1-M}\right) \qquad (5)$$

Figure 2 is a plot of P versus Δ t for different modulation values.

It must be emphasized that this expression only represents an ideal upper limit. It assumes that every photon absorbed from the transmitter beam immediately produces a metastable atom. It does not take intc account the depopulating effect of the receiver beam (which must necessarily irradiate the element continuously). In any process of induced absorption in which the metastable energy levels are populated by removing atoms from excited states, the time constants of these intermediate processes must be taken into account. Equation 4 is only useful in that it defines the problem boundaries.

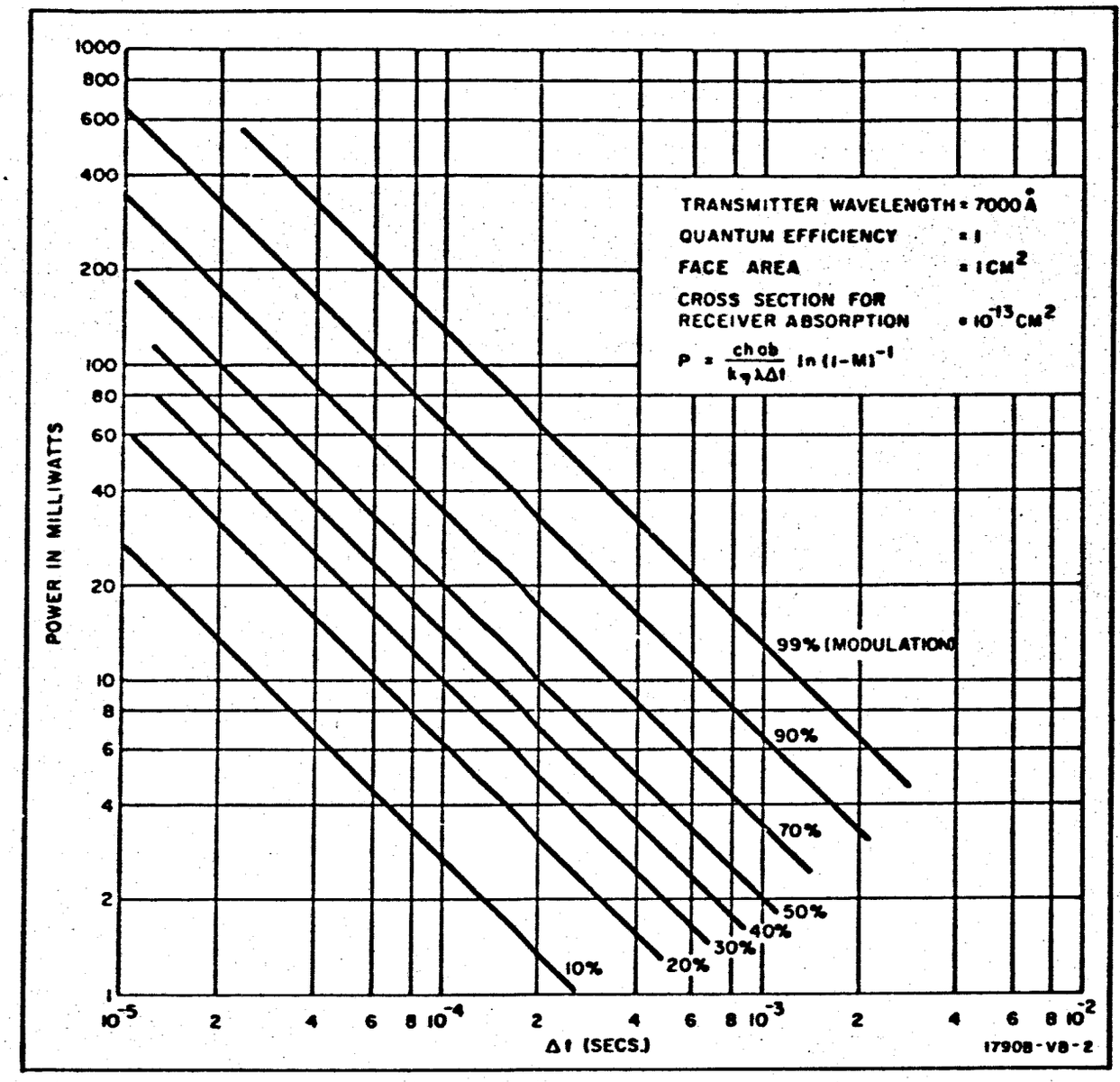

Figure 2. Power vs Δt for Different Modulation Values

2.3 GENERAL MATHEMATICAL FORMULATION

It is possible to set up a general system of equations which expresses induced absorption in terms of intensities, transition probabilities, diffusion coefficients, and population densities. A solution to these equations can, in principle, be obtained which will express modulation of the receiver beam in terms of modulation on the transmitter beam. For cases in which the number of energy levels significantly involved in the process is large, the system of equations can become very complex. In these cases, rigorous solutions will be extremely involved, so a means is usually sought by which to simplify the entire solution process. A typical example is given later in this report.

A reasonable mathematical formulation begins with setting up rate equations for the energy levels involved in the process; i.e.:

$$\dot{n}_1 = I_1 B_{12} n_1 + I_1 B_{21} n_2 + \sum_{j \neq 1} a_{j1} n_j - \sum_{j \neq 1} a_{1j} n_1 + D_1 \nabla^2 n_1$$

$$\dot{n}_2 = I_1 B_{12} n_1 - I_1 B_{21} n_2 + \sum_{j \neq 2} a_{j2} n_j - \sum_{j \neq 2} a_{2j} n_2 + D_2 \nabla^2 n_2$$

$$\dot{n}_3 = \sum_{j \neq 3} a_{j3} n_j - \sum_{j \neq 3} a_{3j} n_3 + D_3 \nabla^2 n_3$$

. . . . . .

$$\dot{n}_k = -I_2 B_{k\ell} n_k + I_2 B_{\ell k} + I_2 B_{\ell k} n + \sum_{j \neq k} a_{jk} n_j - \sum_{j \neq k} a_{kj} n_k + D_k \nabla^2 n_k$$

$$\dot{n}_\ell = I_2 B_{k\ell} n_k - I_2 B_{\ell k} n + \sum_{j \neq \ell} a_{j\ell} n_j - \sum_{j \neq \ell} a_{\ell j} n + D_\ell \nabla^2 n_\ell$$

where the n_i are population densities of the involved energy levels, I_1 and I_2 are the intensities of the transmitter and receiver beams respectively,

the B's are Einstein coefficients of induced emission,

the D's are diffusion coefficients, and the a's are transition probabilities.

The a's of course, represent transition probabilities per unit time due to a large number of possible processes, some of which are collisions of all types, (with atoms of the same or different kind, container walls, etc.),

spontaneous decay processes, phonon interactions, etc. Note that each of the equations contains two terms involving sums. The sum $\sum_{j=i} a_{ji} n_j$ represents all processes by which the i^{th} state can be populated as a result of transitions from other energy levels. The second sum $\sum_{j \neq i} a_{ij} n_i$ represents all ways in which the i^{th} energy level can be depopulated as a result of any transition from the i^{th} level. Since n_i is independent of this sum, it can be removed from the summantion sign;

$$\sum_{j \neq i} a_{ij} n_i = n_i \sum_{j \neq i} a_{ij} = \frac{1}{\tau_i} n_i \qquad (5)$$

where

$$\sum_{j \neq i} a_{ij} = \frac{1}{\tau_i} = \sum_{j \neq i} \frac{1}{\tau_{ij}}$$

is clearly identified with the average lifetime of the i^{th} state when transitions to all other energy levels are considered. By definition, this term would be zero ($\tau_i =$) for the ground state.

The diffusion terms appear in order to account primarily for diffusion processes in gases and conduction bands of solid state materials. Simplifications can sometimes be made with respect to these terms since diffusion terms for different energy levels of the same gas would be expected to be equal, whereas in solid state materials the diffusion coefficient might be nonvanishing for only one term; i.e., the conduction band population. Also, some states have such short lifetimes that diffusion becomes meaningless.

Note that the effects of incidence of the transmitter and receiver beams have been associated with levels 1, 2, k, and ℓ. It appears reasonable that levels 1 and 2 (the ground and first excited state) be associated with the transmitter beam, while generality has been expressed mathematically by assigning arbitrary levels to the receiver beam. For an efficient communication system, there should be as few as possible intermediate levels.

To these ℓ rate equations, two more equations must be added. These two added equations express absorption of the twc optical beams and are of the form

$$\frac{I_{ij}}{x} = - IB_{ij}\, h\nu\, n_i + \left\{ IB_{ji}\, h\nu + A_{ji} \right\} n_j, \qquad (6)$$

where B_{ij} and B_{ji} are coefficients of induced abscrption and emission, and A_{ji} is a coefficient of spontaneous emission between the j^{th} and i^{th} states.

Evidently, from this set of $\ell + 2$ equations, the functional dependence between I_1 and I_2 can be obtained - in theory at least. This method is applied to a specific case later in this report.

Optical pumping methods are obviously numerous. Little need be said, for instance, about the many methods of producing laser action - a closely related field. The two methods for achieving passive modulation transfer described in this report only scratch the surface of possibilities.

3. PASSIVE LIGHT MODULATION USING ALKALI HALIDES

3.1 INTRODUCTION

In order to satisfy the completely passive modulation transfer goal of this program several solid state modulation approaches were considered. One of these approaches using an alkali halide is outlined below.

At the outset of this experiment, it seemed possible, at least in theory, to modulate one light beam with another using permanently colored alkali halide crystals. When using this approach the photons contained in one light beam destroy a number of F-centers in the modulating medium. The decrease in the number of absorbing centers results in an increase in the transmission coefficient of the medium. Thus, in the crystal the intensity variation (in the case at hand, on and off) of the first beam is transferred to the second beam and modulation is accomplished. The percent modulation is proportional to the fraction of F-centers destroyed.

3.2 BRIEF HISTORY OF ALKALI HALIDES

Many polar crystals, when heated in the vapor of one of their constituents, will acquire an excess of that constituent. This stoichiometric unbalance will change the transmission properties of the crystal, since altering its (band) structure will modify the previously existing allowed transitions. Also, in some cases, entirely new absorption bands will be introduced by this method.

A substantial band in the visible and another band at a longer wavelength was discovered by Ottmer in alkali chlorides and fluorides after heating these samples in the vapor of an alkali metal. Subsequently, the properties of these colored halides were studied in great detail by R. W. Pohl and his coworkers. Pohl names the absorption band, F band, and the centers causing the absorption F-centers (Farbzentren in German). Chemical methods showed that these crystals have an excess of metal of up to one part in ten thousand.

The F band is associated with a stoichiometric excess of metal in the halide and, according to the theory of absorption, it should be due to an electronic transmission from a ground state to an excited level. Through further experimentation a broad factual base was obtained concerning these crystals and theoretical approaches were attempted to explain the details of the absorption bands; i. e., their positions, shape, and temperature dependence.

Among the earliest theoretical approaches, two will be mentioned here. According to one approach, the absorption bands are due to excess metal in regular sites, while according to the other, metal ions in interstitial positions cause the bands. In the first approach the excess metal is in a regular site, decreasing the number of metal (positive) ion vacancies. The decrease in the number of positive ion vacancies increases the number of negative ion ones, since the rate of generation of these defects is approximately the same as before doping, but due to the decrease of positive ion vacancies, the recombination rate of the negative ion vacancies is slowed down. This causes an increase in their number. In case the ion is in a usual site, due to the increase of the negative ion vacancies, the chances of an electron getting captured by these vacancies are enhanced. The absorption band is then due to the excited states of the electron in this hole. According to the second approach, if the ion is in an interstitial position, the observed color is due to the transition of its orbital electron. The respective entropies for regular and interstitial sites are $k \log \frac{N!}{n!\,(N-n)!}$ and $k \log \frac{(N' + n)!}{n!\,N!}$, where n is the number of ion pairs per unit volume, N the number of interstitial positions and N' is the number of ion pairs. Since n is much less than either N or N', both of these expressions reduce to $-N\,kc \log c$, where $c = \frac{n}{N}$ or $\frac{n}{N'}$, respectively. Entropic considerations therefore will not satisfactorily resolve the problem. A belief that the first possibility is correct, that is, the metal ion occupies a regular site, is based on the evidence that the same bands can be obtained in these salts when irradiating them with X-rays. The low energy X-rays cannot displace ions from their sites, but they can, mainly by the Compton effect, knock electrons from their orbits. These electrons can travel long distances

in the lattice and then be captured by a negative ion vacancy, since there is a number of these always present in the lattice. They are then confined to the vicinity of this vacancy and can be excited from the ground state into an excited one. However, low energy X-rays do not have enough energy to displace an ion from its regular position to an interstitial location; this implies that the first approach is the correct one.

The method of additive uniform coloration throughout the crystal is accomplished as follows. As the heated metal vapor is deposited onto the surface of the halide crystal, some of it combines with a metal ion vacancy and depletes the positive ion vacancies at the surface. Due to this concentration gradient, positive ion vacancies diffuse from the bulk of the material to the surface where they are used up. The decrease of these vacancies in the bulk results in an increase of the negative ion concentration throughout the crystal, since reducing one of these constituents will reduce the recombination rate of vacancies of opposite sign. Also, when a metal atom combines with the positive ion vacancy, it liberates an electron which can then relatively quickly diffuse through the crystal. There is now an enhanced chance for the electrons to be trapped by these negative ion vacancies, resulting in an F-center. Since the diffusion of vacancies is appreciably faster than the diffusion of the metal atom (or ion) this process takes only a few hours at temperatures close to the melting point of the crystal.

It can be shown theoretically and has been experimentally verified that the doping level of halides can be controlled by the temperature of the halide and metal vapor system. The level of doping can then be predetermined and, once it is obtained (provided that the absorption coefficient of the center is known), the thickness of the crystal can be calculated for a desired amount of transmission. A brief outline of these considerations is given in Appendix I

3.3 ANALYSIS OF EXPERIMENTAL DATA

The theory of F band formation and predictions relating to the peak halfwidth, shape of the absorption curve, and the temperature dependence of these parameters was recently reviewed by Markham. The basic problem is how the electron transition from a ground to an upper state influences the normal vibrational modes of the crystal. Fundamentally, the capture of an electron modifies its surroundings through several interactions. When these interactions are broken down into categories in order to be able to treat them mathematically, it appears that the most important ones are the following. First, the electron introduces a force causing a nonuniform shift of the nuclei (figure 3). This is analogous to the compression of a spring and causes an energy storage. Second, due to the above shift the distances between nuclei, and thus the forces between them, are changed. This will result in a change of the angular frequencies of the lattice. At 0°K the probable position of the ion is given by a gaussian surface. Trapping will cause a broadening or narrowing of this distribution. The third effect is due to the phonon-electron interaction. That is, the electrons and nuclei adjust their position in such a way as to make the total energy a minimum. If time independent perturbation theory is used to describe this state, the position of the electron depends on the position of the nuclei (it is always adjusted to a minimum) leading to the dependence of the electronic wave functions on the nuclear wave functions. These functions are no longer simple independent products, making the Schroedinger equation no longer separable by simple methods, and the solution is not made out of simple products of independent wave functions. These interactions determine the location of the center of the band, its halfwidth, shape, and temperature dependence. Since these quantities will depend on the instantaneous position of the nuclei and electron immediately before and after the transition, the statistical location of these particles, the energies associated with them, and the transistion probabilities accompanying these positions are fundamental ingredients of the problem.

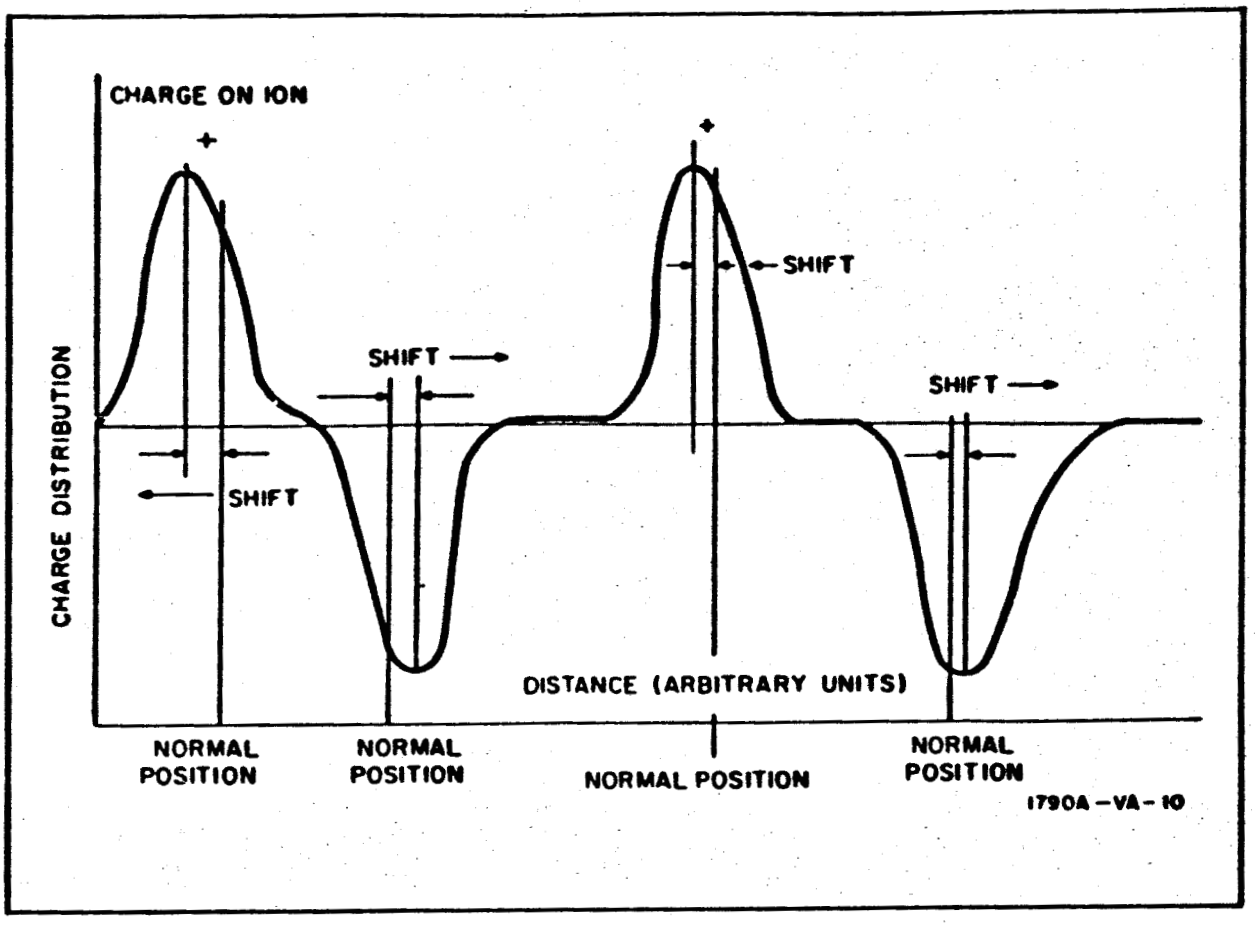

Figure 3. Lattice Distortion Due to a Trapped Electron (From Markham, Not Drawn to Scale)

The formal theory will not be repeated here except in a brief outline. It can be found in more detail in the article by Markham.

The complete Hamiltonian per unit volume for a solid is given by $H = T_e + T + V(R)$, where T_e is the kinetic energy of electrons, T, the kinetic energy of the nuclei, and V(R) the total potential energy. T is given by

$$-\frac{\hbar^2}{2} \sum_R \frac{1}{M_R} \nabla_R^2 \ldots\ , \qquad (7)$$

where M_R is the nuclear mass.

The Born Oppenheimer technique assumes that, if R is fixed, the eigenfunctions, $\phi_h(R)$, and eigenvalues, $\epsilon_n(R)$, associated with $h_e(R) = T_e + V(R)$

are known. A second set of eigenfunctions is obtained using

$$h_v(R) = T + \epsilon_n(R) - \epsilon_n(R_n) \tag{8}$$

where R_n is given by

$$\left.\frac{\partial \epsilon_n}{\partial x_\alpha(k)}\right|_{R_n} = 0, \tag{9}$$

h_v then becomes

$$T + \frac{1}{2} \sum_{\alpha,\beta,k,\ell} \left[\frac{\partial^2 \epsilon_n}{\partial x_\alpha(k)\ \partial x_\beta(\ell)}\right]_{R_n} \Delta x_\alpha(k)\, \Delta x_\beta(\ell) \tag{10}$$

where $\Delta x_\alpha(k)$ is the displacement relative to R_n. If normal coordinates are now introduced, h_v becomes

$$\frac{1}{2} \sum_{j}^{3N} (p_j^2 + \omega_j^2 g_j^2). \ldots \tag{11}$$

where the ω's are solutions of the secular determinant

$$\left| \frac{1}{(M_k M_\ell)^{1/2}} \left[\frac{\partial^2 \epsilon_n}{\partial x_\alpha(\beta)\ \partial x_\beta(\ell)}\right]_{R_R} - \omega^2 \delta_{\alpha\beta} \delta_{k\ell} \right| = 0 \tag{12}$$

The individual terms comprising h_v correspond to solutions of the simple harmonic oscillator with eigenfunction $_{nj}$ and eigenvalues $\hbar\omega\,(V_j + \frac{1}{2})$. The total eigenfunction h_v is a product of all these and is denoted by χ_n. n denotes the electronic state, v_j is the vibrational quantum number in the jth state, and v_t is the sum of v_j. The analysis is concerned only with an upper and lower state and so n will denote either the upper or the lower state. The corresponding eigenfunctions and eigenvalues will be denoted by ϕ, χ and ϕ', χ'. It is the transitions between these states using the above eigenfunctions and eigenvalues with which this analysis is concerned. The essential problem is to find or approximate the eigenfunctions to the original Hamiltonian $H = T_e + T + V(R)$. Once these functions are known for the ground state and the

excited state the dynamical variables (energy, momentum, etc.) of interest are obtained from

$$\int \phi'^{*} O \phi \, d\tau = \langle \phi | O | \phi \rangle ,$$

with the integration over all space (covered by the eigenfunctions).

The respective approximations will not be reviewed here and only the results will be given for the case of KCl.

The broadening of the lines determined by the above process is due to the position of the ions around the excited electron, since the optical activation energy will depend critically on this configuration. Smaller contributions are also due to the Heisenberg principle, which for levels with a finite lifetime gives an uncertainty in the value of energy. Interaction between centers also may cause some broadening; temperature dependence of broadening is due to the fact that during optical transitions the selection rules for v_j's are relaxed. The comprehensive detailed principle of broadening is not fully understood in these materials, but it is known that broadening results from removing most of the degeneracy in the levels caused by extended overlapping of electron and ion wave functions.

Experimentally, the absorption curves, $a(\epsilon)$, are not simple analytical curves (cannot be well fitted with closed functions). In order to deal with these curves, several symbols and definitions are useful, such as

ϵ_m, the energy where a is maximum,

ϵ_r, and ϵ_v the half-maximum on red and violet side,

$M_n = \int_0^\infty a(\epsilon) \, \epsilon^n \, d\epsilon$, the nth moment,

$\overline{\epsilon} = M_1/M_0$, the average

$m^2 = \frac{1}{M_0} \int_0^\infty (\epsilon - \overline{\epsilon})^2 \, a(\epsilon) \, d\epsilon$, and

$H = \epsilon_v - \epsilon_r$, the halfwidth

Comparing these quantities for KCl with the values computed for a Gaussian, Lorentzian, Double-Gaussian, and Pekarian function, it was found that the Pekarian curve fits the asymmetric absorption curve the closest. The Double-Gaussian, with its long wavelength side wider than its violet side, can also produce a close fit, but it is outside the experimental error in case of KCl data. The theory of the line shape will not be reproduced here. It can be found in its current state of refinement in Markham's article.

The general shape factor is given by:

$$G_h(\nu) = \frac{1}{2\pi} \int_{-\infty}^{\infty} e^{-i(\nu - \nu_{\mu g})t} \prod_j F_j(t)dt$$

The low temperature approximation is given by $G_l(\nu) = \frac{S^p}{P!}$ while the high temperature shape is given by $G_h(\nu) = \frac{1}{(2\pi Z)^{1/2}} \exp\left(Z - \frac{p^2}{2Z} + \frac{p}{2} \ln\left(1 + \frac{1}{\bar{\nu}}\right)\right)$.

The low and high temperature maxima occur at:

$$p_l = S \text{ and } P_h = 1/2\ Z \ln\left(1 + \frac{1}{\bar{\nu}}\right) = \frac{\hbar\omega Z}{2k\theta}$$

where $p = (\nu - \nu_{\mu g})/\omega$, ν being the frequency of the photon and ω that of the phonon. S, (the Huang - Rhys factor), is $1/2 \sum_j \frac{e^2}{\omega_j^3 \hbar}$, $Z = 2S\left[\bar{\nu}(\bar{\nu} + 1)\right]^{1/2}$, $\bar{\nu} = 1/2\left[\coth\frac{\beta}{2} - 1\right]$, $\beta_j = \frac{\hbar\omega_j(g)}{k\theta}$, and θ is the temperature in degrees Kelvin, $\lambda_j = \beta_j + i\omega_j t$, a variable in F_j. The expression for F_j is

$$2 \sinh 1/2\ \beta_j \iint \left\{ \sum_{v_j} \exp\left[-(v_j + \tfrac{1}{2})\lambda_j\right] \chi_j(q_j)\, \chi_j(q_j') \right\} \times$$

$$\left\{ \sum_{v_j} \exp\left[-(v_j' + \tfrac{1}{2})\mu_j\right] \chi_j'(Q_j)\, \chi_j'(Q_j') \right\} dq_j\, dq_j' \ .$$

The temperature dependence of P_h is given above, while the temperature dependence of H is $(5.545)^{1/2} \hbar\omega Z^{1/2}$. At high temperatures H becomes $(11.090\ S\ k\ \hbar\omega)^{1/2}\theta^{1/2}$. According to P_h, the peak of the absorption curve varies with θ as $\frac{Z}{\theta}$. Z here is a function of θ, and it turns out that $\frac{Z}{\theta}$ is an insensitive function of T. Validity criteria for high and low temperatures seem to indicate that P_h holds above room temperature and p_l is applicable around liquid helium temperatures.

Comparing Pekar's parameters with the experiment performed on KCl at 300° K, the calculated H is 0.43 ev compared to 0.35 ev for the experimental value. The experimental figure is an average of data obtained from the most recent investigators. At 0° K the calculated H is 0.30 ev compared with the experimental value of 0.16. Also, the equation $H^2 = H^2(0) \coth \frac{1}{2}(h\omega/k\theta)$ obtained from Pekar's analysis suggests plotting $\frac{H}{H(0)} = \text{arc coth } h\omega/k\theta$. H(0) is the half-width at 0° K and can be approximated from measurements at 4° K. The straight line passing near the origin (figure 4) is an indication of the approach taken, and the approximations used. Further, it shows that there is one effective mode and that it can be utilized in the development. There are other expressions which can be extracted and plotted using Pekar's theory. Several investigators used these approaches, but they will not be presented here since the straight line plot above is as conclusive as any of the other methods.

Summarizing, a theory was set up jointly by several investigators based on a physical picture of two bound states and a simple model; for this picture some of the calculations could be carried out to conclusions. The broadening, briefly, is due the removal of degeneracy of the bands by narrow sub-bands, due to the uncertainty principle, due to center-to-center interaction, and due to the dispersion of normal modes because of disruption of periodicity. The resulting shape of the curve is due to the time of transition, and therefore the terms determining it come from phonon considerations, the photons

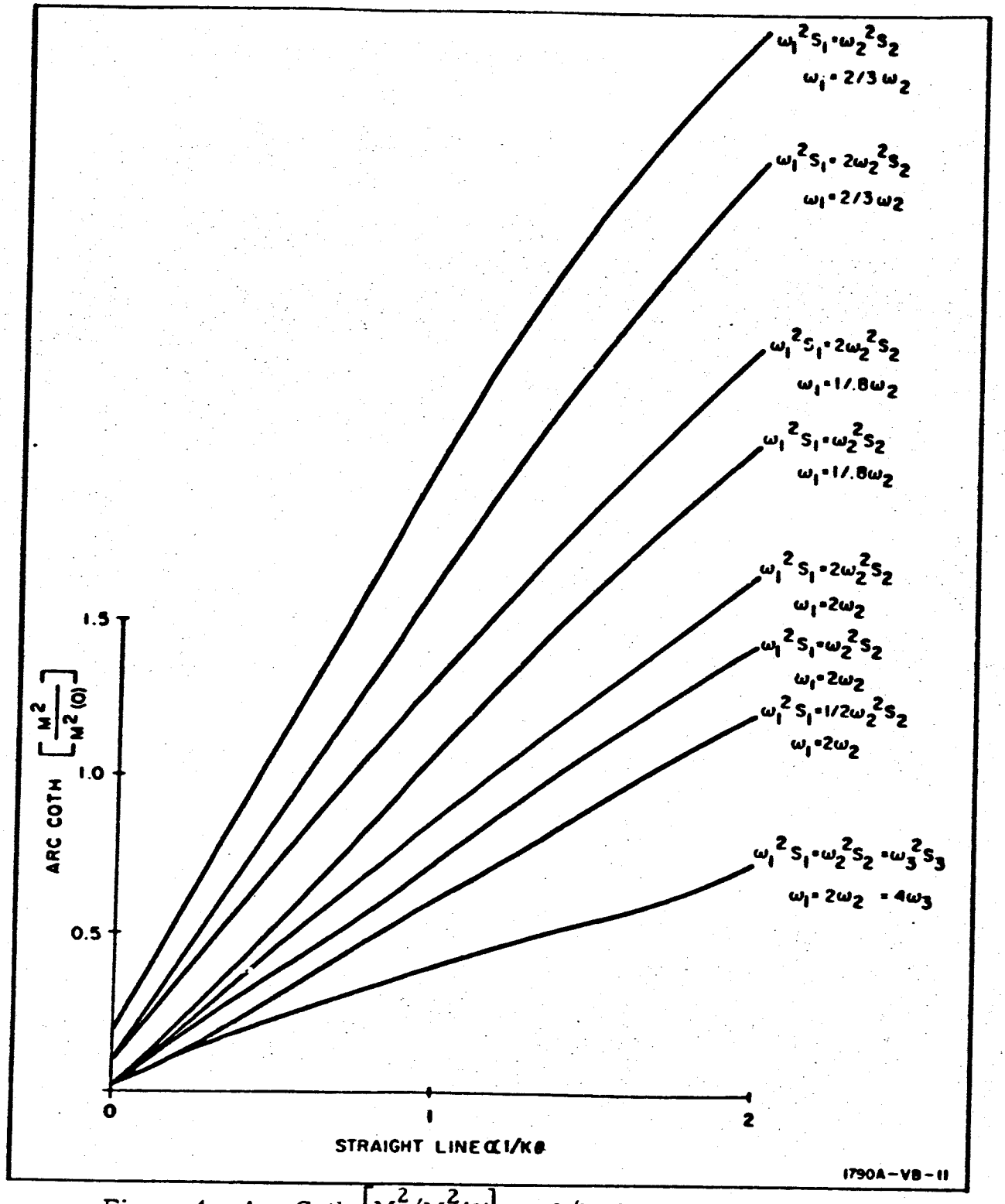

Figure 4. Arc Coth $\left[M^2/M^2(0)\right]$ vs $1/k\theta$ Vindicates Theoretical Approach Taken (From Markham)

playing only an assisting role. Figure 5a shows the potential energy at absolute zero in the ground and the excited state. The transition probabilities are shown in figure 5b. The result is an asymmetric curve resembling the F-center in KCl. Once the comparison between experiment and theory is extended to higher temperatures, additional approximations have to be made and the agreement between theory and experiment becomes less satisfactory. Also, the curve becomes more symmetric and, to the accuracy of the calculations, the model does not explain, for example, the difference between E^e and E^a. The error is over 20 percent. Here E^a and E^e are the activation energies for absorption and emission.

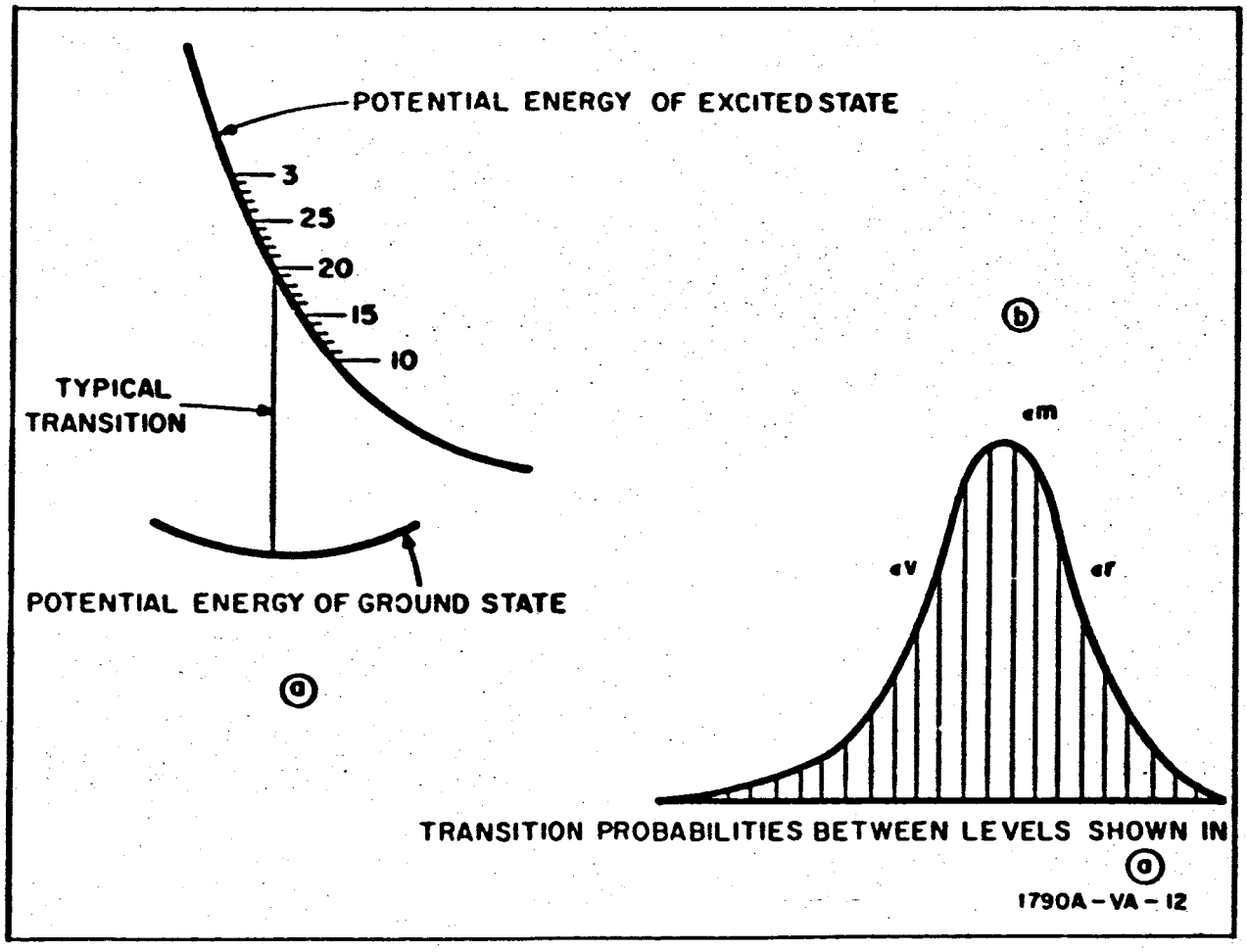

Figure 5. Illustration of Band Formation

It also should be pointed out that all data used above for comparing the theory with the experiment was taken with KCl, and no data are availabie on other halides to compare the theoretical predictions of this approach with experiment.

3.4 APPLICATION OF THE THEORY

On the long wavelength side of the F band there is another absorption region called the F' band. According to theory this band consists of two electrons around a negative ion vacancy. When this center absorbs a quantum of energy the electron in the upper state is excited and leaves the vicinity of the center. The center then is left with one electron and thus is an F-center. The converse of this process is also possible, since using F light, an F electron can be liberated and attached to another F-center. This will give an F'-center. These two reversible processes suggest a modulation scheme depending on interconversion of F- and F'-centers. Actually, to explain the temperature dependence of the interconversion efficiency of these two centers a third level, situated slightly below the conduction level, is introduced. It is postulated that the electron occupies this intermediate level below the conduction level for some time before it is either excited into the conduction band or drops back to the ground state. This postulate is necessary to explain the drop in conversion efficiency with the drop in temperature. According to Gurney and Mott, a quantum of light removes the electron from the negative ion vacancy, but does not separate it from the defect completely. The electron is put into a level just below the conduction band. Later a phonon can impart enough energy to the particle to separate it completely from the binding center and put it into the conduction band. The number of electrons released per absorbed quantum is $\eta = \frac{B}{A+B}$, where A and B are probabilities per unit time that the electron will drop back to the center or be freed by a phonon respectively. A is the Einstein coefficient for spontaneous transition, given by, $E_o = 10^{10} f \left(\frac{h\nu}{13.54}\right)^2 \approx .5 \times 10^8 \text{ sec}^{-1}$, while B is given by $B_o e^{-E/kt}$.

If B_o and E_o are assigned the proper values, then η will agree with experiment for certain halides in a certain temperature range. Considering the conduction band and the F and F' levels, the following rate equations will describe the process of interconversion for one level to another.

$$\frac{dn_F}{dt} = -nI_F + I_F' + k_V n_V n_E - k_F n_F n_E$$

$$\frac{dn_V}{dt} = nI_F - k_V n_V n_E$$

$$\frac{dn_F'}{dt} = k_F n_F n_E - I_F'$$

$$\frac{dn_F}{dt} = -k_F n_F n_E - k_V n_V n_E + I_F' + nI_F,$$

where n_F, n_F', n_V, n_E are concentrations per unit volume of F-centers, F' centers, negative ion vacancies, and conduction electrons, I_F and I_F' are light absorption rates in the F and F' bands (photons/sec cm^3), k_F and k_V are the capture coefficients for F-centers and negative ion vacancies (cm^3/sec), and η is the photo ionization efficiency of the F-center. These equations can be solved for certain conditions, and these solutions were obtained for special cases by Costikas and Grossweiner, which need not be repeated here.

Suppose an alkali halide crystal is colored by radiation or by additive methods to contain a specific number of F- centers. Then by illuminating with light in the F absorption band, F'-centers will be created and the absorption of F' light will increase. At the same time the absorption of F light will decrease. On the other hand illumination with F' light will increase the absorption of F light and decrease absorption of F' light. Thus, if the material in front of a corner cube is made out of a halide having its absorption bands at a proper wavelength, and if it is illuminated from A with strong F light, its absorption of F' light from B will increase. When C is not illuminated from A its absorption of F' light will be constant and possibly slightly decreasing

due to the monitoring F' light intensity. In this manner information transfer from A to B via C can be accomplished. By having a filter in front of C, transmitting at both the F and F' wavelengths, but blocking at all other frequencies, the effect of stray light on the operation of this system can be eliminated.

Since this scheme, at least in theory, suggested a passive modulation transfer mechanism, an experimental program was conducted. The description of this experimental work follows.

3.5 EXPERIMENTAL SETUP

3.5.1 Sample Preparation

Potassium iodide was chosen as the halide for the modulating medium, since its absorption band at room temperature peaks within ±50 Å of the ruby laser wavelength (6943 Å). The material was obtained from Harshaw Chemical Company and irradiated at the Westinghouse Research Laboratories to introduce the colored centers. Even though the radiation-introduced centers are not as stable as those due to additive coloring, it was decided that they would be used, since their method of preparation is not as elaborate as that of additively colored ones. Also, sample preparation after coloration is eliminated.

For additively coloring a halide crystal, a special setup is necessary in which the sample can be heated together with an alkali metal vapor at a specific temperature for a predetermined length of time. The lining in this enclosure must be made of a special metal to avoid contamination and the chamber must be provided with a quick release mechanism in order to quench the sample from its diffusion temperature to room temperature in a matter of seconds. This is done by opening the furnace and quickly dropping the hot sample into a tube filled with oil. This rapid cooling prevents the coagulation of F-centers into colloidal globules and makes the sample usable (if it does not develop cracks along its cleavage planes due to this thermal shock). The surfaces of the samples prepared this way are usually pitted due to the interaction of the hot alkali vapor and the crystal. They also become further contaminated by being dropped into the cooling oil. This hazy pitted surface layer has to be removed by grinding or etching, but since the crystal cannot be exposed to other than the F-center light at room temperature, this operation has to be performed in almost complete darkness.

Irradiation eliminates the need for surface preparation after coloration, since the surface of the irradiated sample is the same after coloration as it was before. This method of coloring consisted of irradiating the prepared sample with electrons from the Van de Graaff generator at the Westinghouse Research Laboratories. After having been cleaved into 1/4 x 1/2 x 1/2-inch pieces and polished, the samples were put into an aluminum envelope. The 0.7-mil aluminum foil used almost hermetically seals the KI crystal, so that it does not absorb any moisture from the air even after months of exposure. In order to get 10 percent transmission with a sample saturated with F-centers (about $10^{17}/cm^3$) coloration to a depth of about 0.01 cm is required, according to $K = N \times 10^{-16}\ cm^{-1}$. Relying on the fact that electrons in the Kev range penetrate about $1 gm/cm^2$ 2 Mev, it was calculated that the beam energy should be about 200 kv in order to go through the aluminum foil and penetrate into the crystal to about 0.02 cm. (The density of KI is about 3.1 gm/cm^3.) Actually, the beam energy had to be increased, since toward the end of the penetration depth, the electron energy is diminished and the coloration effect is decreased. It is suspected that the threshold energy needed to introduce F-centers into halides is about 115 to 130 Kev. Also, the machine window through which the electrons exit is made of 5-mil thick Dural; in addition, these particles have to penetrate about 3/4 inch of air before reaching the crystals. Also, the machine flux at 200 Kev is low and its energy drifts. For these reasons, in order to obtain sufficient coloration reproducible to a depth of about 10 mils, the Van de Graaff was set at 300 Kev. The irradiation time was about 2.5 hours and the integrated amount of charge obtained by a sample ranged from 25 to 40,000 μcoulombs. The resulting F-band, as observed on the Cary Photospectrometer is shown in figure 6.

This highly colored layer is needed because it is advantageous to be able to focus both beams onto each other and have the modulation take place at that point. In case the crystal is uniformly colored (as it can be by using high-energy electron beams which lose only a small fraction of their energy in the crystal), the spot where the modulation takes place is difficult to locate,

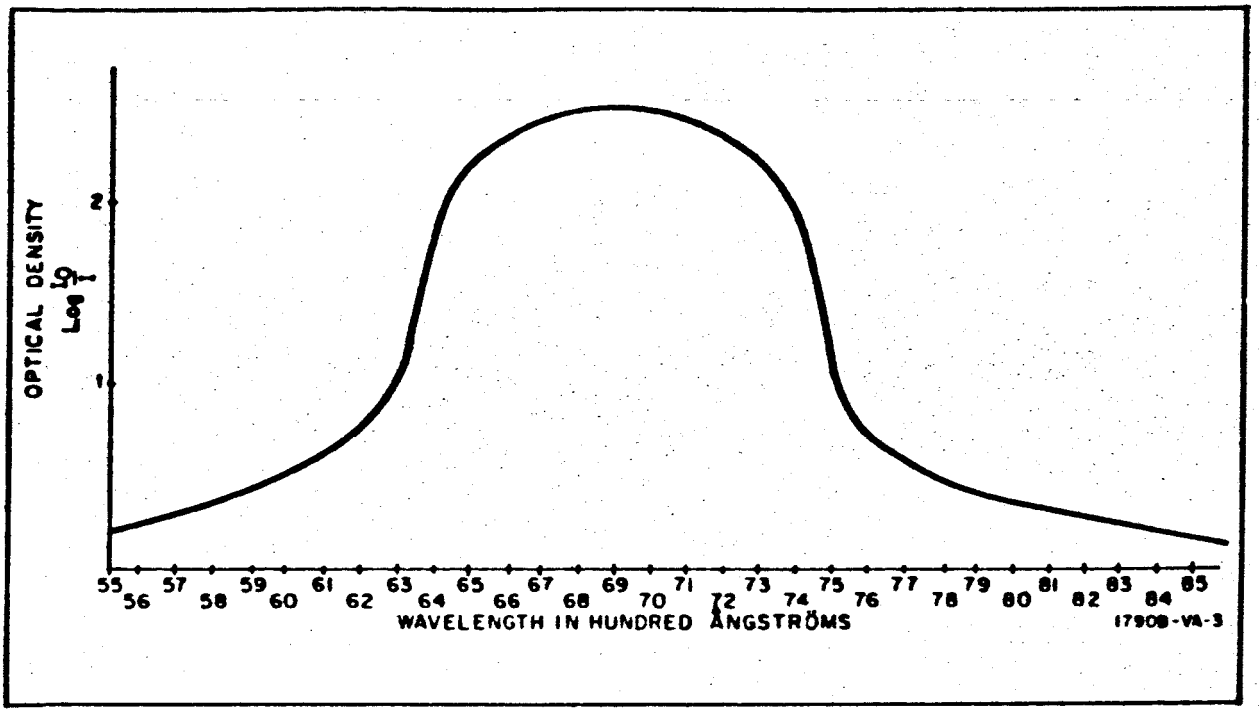

Figure 6. F Band of Irradiated KI Sample

and there is some loss of modulation efficiency, since the absorption of the sample is small at the place where the beams meet and does not present an efficient modulation medium. When the crystal is uniformly colored the two beams impinge at right angles and cross without sufficient interference.

3.5.2 The Dewar

After the sample is prepared it is transferred from the aluminum envelope into the cryostat under a dark red light. This is the only time the irradiated sample sees light at room temperature other than that corresponding to the F or F' bands. The cryostat consists of an outer pyrex envelope with a ground glass opening on the top and a side opening used for evacuating it. On its side it has two pairs of flat windows as shown in figure 7a. The inner part (figure 7b) is made to fit the ground glass joint and through a series of seals it supports the metal sample holder. When operating the unit, the inner enclosure is placed into the outer cne. The liquid nitrogen is poured into its central portion and through conduction the sample holder and sample are cooled. When operating the device it was found that the copper

sample holder did not provide a sufficient conductive path to neutralize the incoming heat by radiation at liquid nitrogen temperatures. Therefore, to reach this temperature after the enclosure was evacuated the pumping was discontinued and some nitrogen gas was allowed to leak into the enclosure at the thermocouple lead seal. This nitrogen gas inside the enclosure provided sufficient heat transfer between the sample and the kovar containing the liquid nitrogen so that 93°K could be achieved in a relatively short time. Dry argon was blown over the windows to prevent frosting (figure 8). The temperature was measured with a copper constantin thermocouple, and a Leeds and Northrup K-2 potentiometer. The joint between the thermocouple wires and the wires leading to the potentiometer was held at 0°C.

The dewar containing the sample was mounted between three 1/2-meter optical benches. The benches were clamped together and fine adjustment was provided for optical alignment.

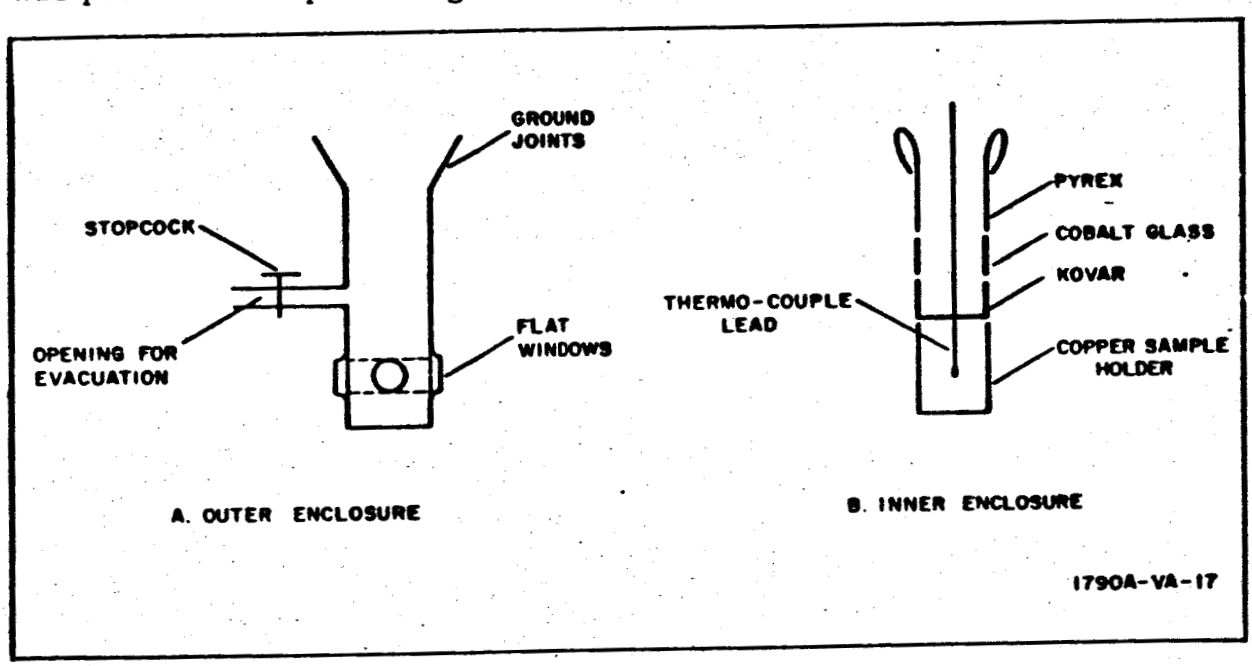

Figure 7. The Dewar

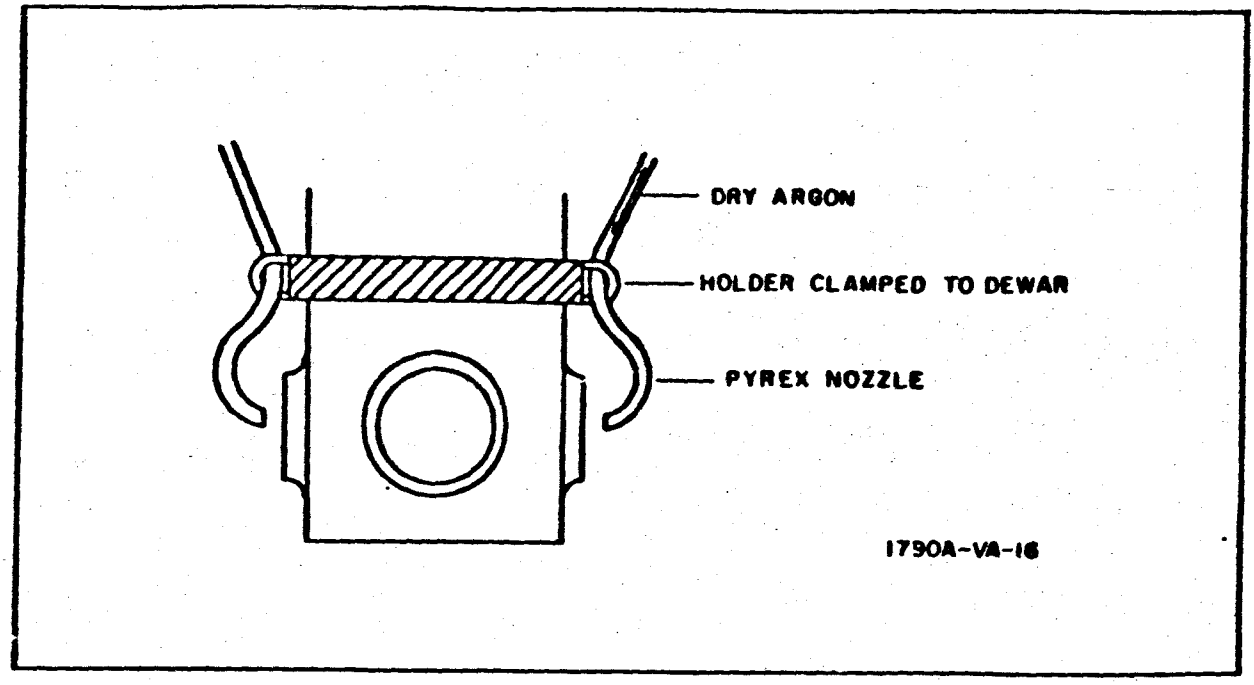

Figure 8. Preventing Frost on Dewar Windows

3.5.3 Equipment

The dewar containing the sample forms the center of the system. The block diagram of this setup is shown in figure 9, along with the description of the necessary equipment to perform the experiment.

The basic framework of the system consists of three optical benches and the dewar all clamped together with provisions for optical alignment. The individual pieces of equipment necessary for operation were mounted on riders, which in turn were clamped to the benches. For identification purposes the three benches of the system were designated 1, 2, and 3 as in figure 9. Briefly, the source is filtered by the bandpass filter and then imaged by two lenses onto the sample through the cryostat window (bench 1). The infrared illumination is provided on bench 3, while the light is collected

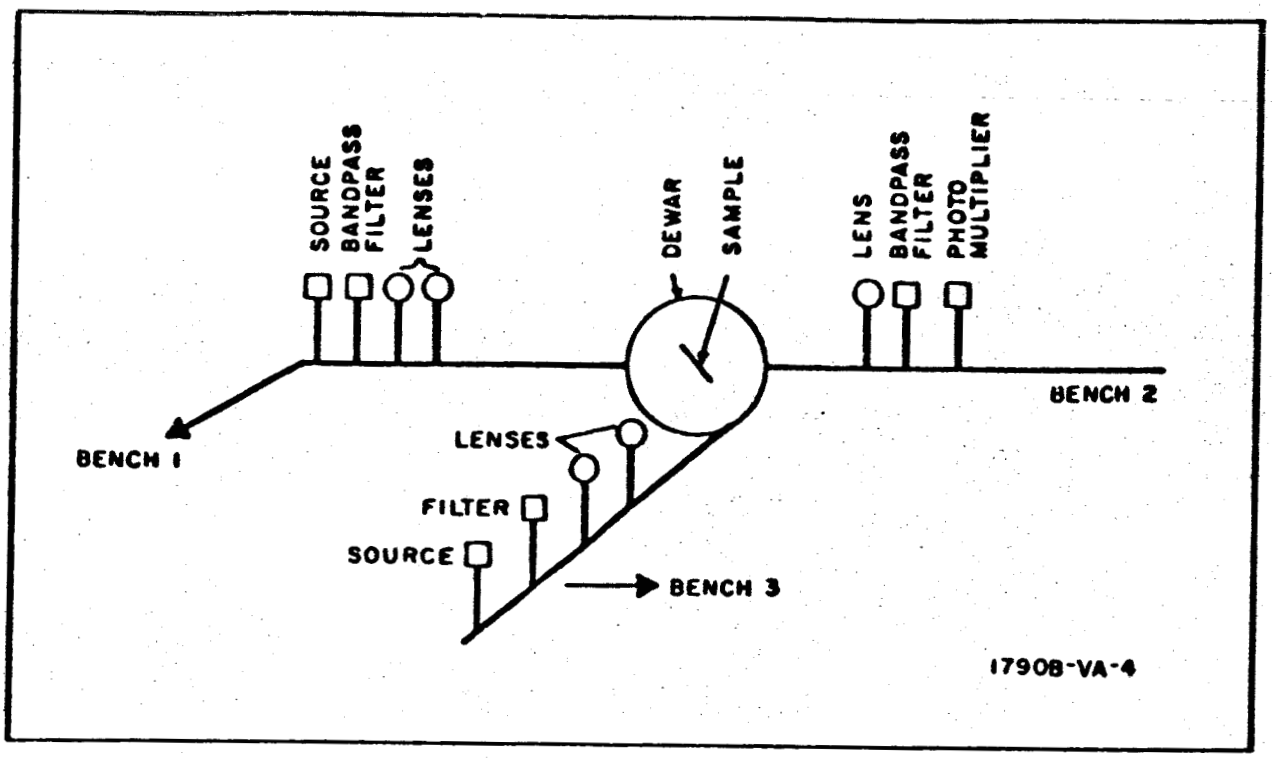

Figure 9. Block Diagram of the System

onto the photomultiplier through a matched bandpass filter (bench 2). The output of the multiplier is displayed on an oscilloscope.

Automobile bulbs and 12-volt batteries were used to eliminate any ac ripple due to partial cooling of the filament at the time of current mode. The bulbs were housed in aluminum enclosures with an opening in the front. The filaments of the bulbs were focused by two f/9 achromatic lenses in order to optimize the optical speed of the system. The filters were placed at the openings on the aluminum boxes so that only light of the desired wavelength was passed. Transmission was measured to be 70 percent at 6943 Å and fell to practically zero at 85 Å from the peak. The transmission curves taken with the Carey recording spectrophotometer showed that on the long wavelength side this filter blocked only out to about 8000 Å. For this reason additional long-wavelength blocking filters were used in conjunction with the 6943 Å units. The difference between transmission with and without the blocking filters is shown in figure 10 and 11. The filter in front of the source was necessary to

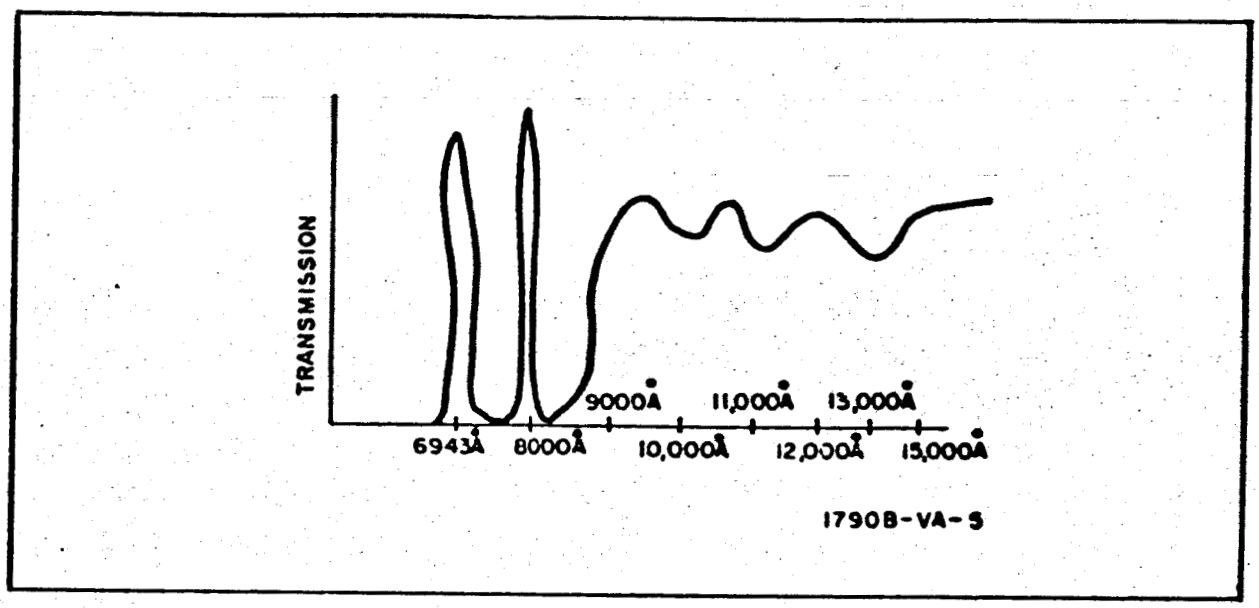

Figure 10. 6943 Å Bandpass Filter Without Long Wavelength Blocker

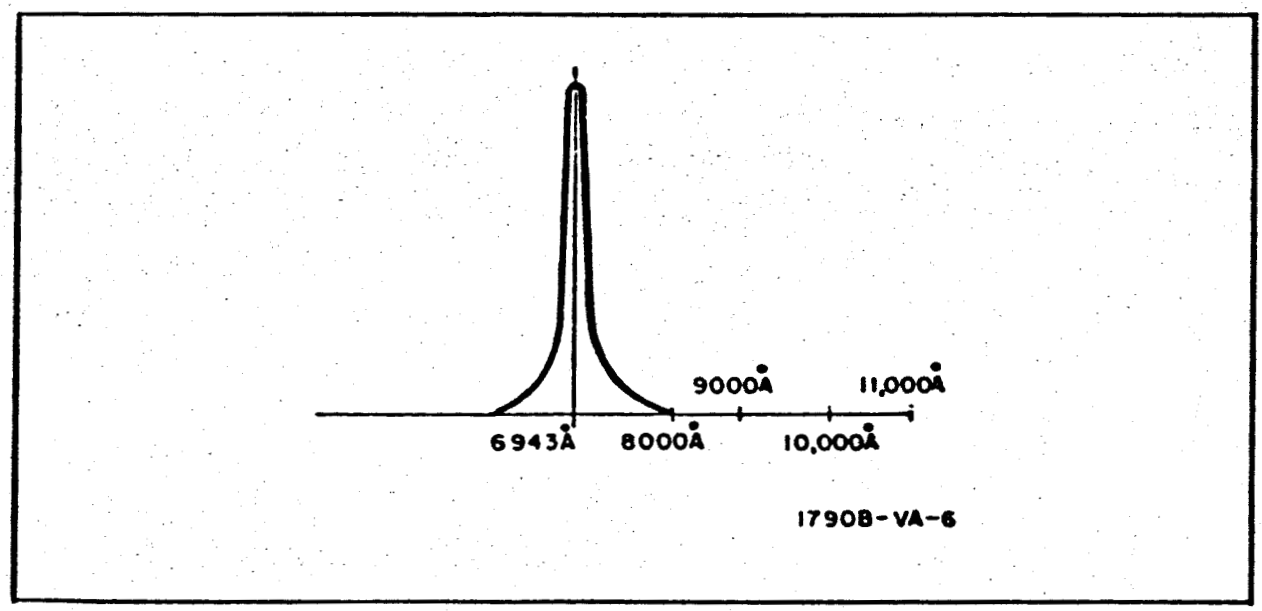

Figure 11. 6943 Å Bandpass Filter With Long Wavelength Blocker

obtain a narrow spectral width in the F region of potassium iodide, while the filter in front of the photomultiplier served to prevent any stray light from reaching the detector. The infrared high-pass filter (bench 3), obtained from Infrared Industires, provided the infrared energy to activate the F' band of KI.

The photomultiplier was a DuMont type K 2190 having an S-20 photocathode. It had a 1-1/4 inch end window and 10 dynodes and was powered by a series of 350-volt batteries enclosed in an aluminum chasis in order to eliminate any power supply ripple or other high-frequency noise. The appropriate voltages were distributed to the respective dynodes by a bleeder. When the photomultiplier was operated in conjunction with a Tektronix L-type plug-in unit or with an L plug-in unit and a Type 122 Tektronix preamplifier, the noise level was less than 50 microvolts. This noise contribution came from the photomultiplier.

3.6 OPERATION AND RESULTS

First it was ascertained that there was no crosstalk; that is no light from bench 3 entered the photomultiplier by stray reflections. Next, the 6943 Å F light was barely allowed to activate the photomultiplier. Both the light level and the multiplier outputs were recorded. Then the multiplier tube was blocked and the intensity of the F light was increased for a definite period of time. At the end of the illumination period the F light was set back to the monitoring level (same as at the outset) and the photomultiplier response was noted. It was found that F illumination increased the transmission for the F light. Next, the F light was shut off and the F' light (bench 3) was turned on, illuminating the sample for a definite time. At the end of the interval, the F' light was shut off and the F light was turned on at the monitoring intensity. A decrease in transmission was observed in this case. Typical values for the samples and intensities (proportional to voltmeter reading) are shown in table I.

Similar results were obtained with the use of a flashlamp (Deutsche Elektronik GMBH, Metear) in place of the light source on bench 3. Igniting the flashlamp displaced the base level on the oscilloscope. When the lamp was flashed while the F light was on, the trace on the scope screen moved immediately indicating an instantaneous decrease in F transmission. The trace slowly returned to its original level, indicating a long recovery time. The time to return to the original level depended on the intensity of the F

TABLE I

TRANSMISSION CHANGES IN KI AS A FUNCTION OF F-AND F'-LIGHT INTENSITIES

Initial Voltmeter Reading (mv)	Time of Illumination	F Light	F^1 Light	Final Voltmeter Reading (mv)
18	5 hours	on	off	700
700	2 hours	off	on	500
360	4 hours	on	off	600
600	3 hours	off	on	500

light for the same setting and geometrical position of the flashlamp. The response obtained with this arrangement is illustrated in figure 12.

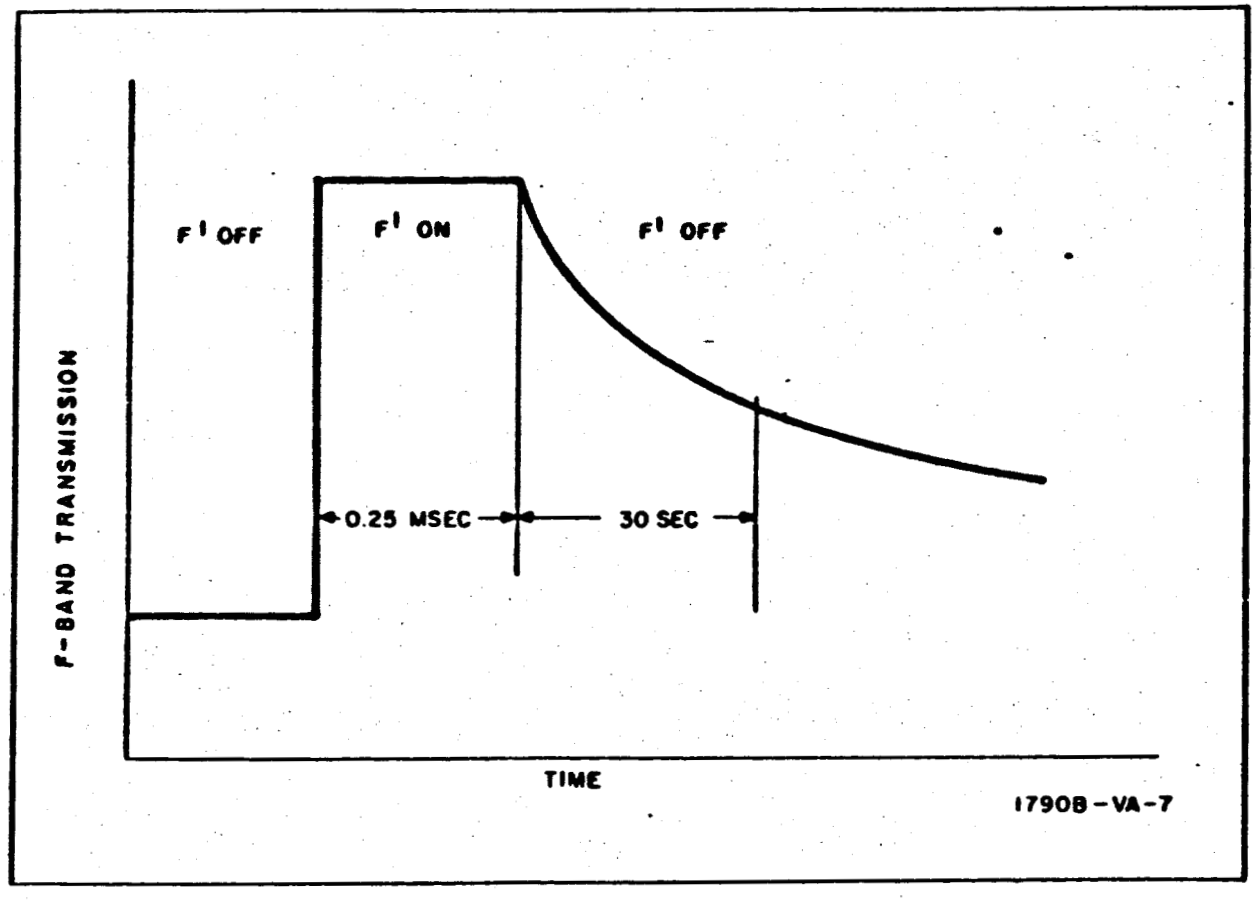

Figure 12. F-Band Transmission During and After Flash Illumination

Modulation was also observed using the Carey Spectrophotometer. Here the sample was placed in its holder and its absorption was checked in the vicinity of 7000 Å. Then the sample was illuminated at 7000 Å and its absorption was checked and was found to decrease. Next, the sample was illuminated at 11,000 Å, and its absorption was checked at 7000 Å. This time the absorption was found to increase. The type of data obtained by this method is shown in figure 13. The three peaks are due to three repeated readings taken after each illumination in order to obtain a certain degree of reproducibility. The readings and curves in all cases served to illustrate the observed effect, though the data is meager and there is no evidence of reproducibility from one crystal to another. All crystals used were commercially available potassium iodide. It is possible that by devoting more time and effort, purer crystals could be obtained, and that by proper doping, the frequency response of this material could be enhanced. It is also possible that diffusion away from the illuminated spot also affected the results. To ascertain whether this is so, the sample-to-spot size area ratio should be varied for different intensities of illumination. Finally, the effects of concentrated sources as compared to diffuse illumination should be examined. After ascertaining these factors, and after an assurance of reproducibility, a definite figure for transmission change per amount of illumination should be obtainable.

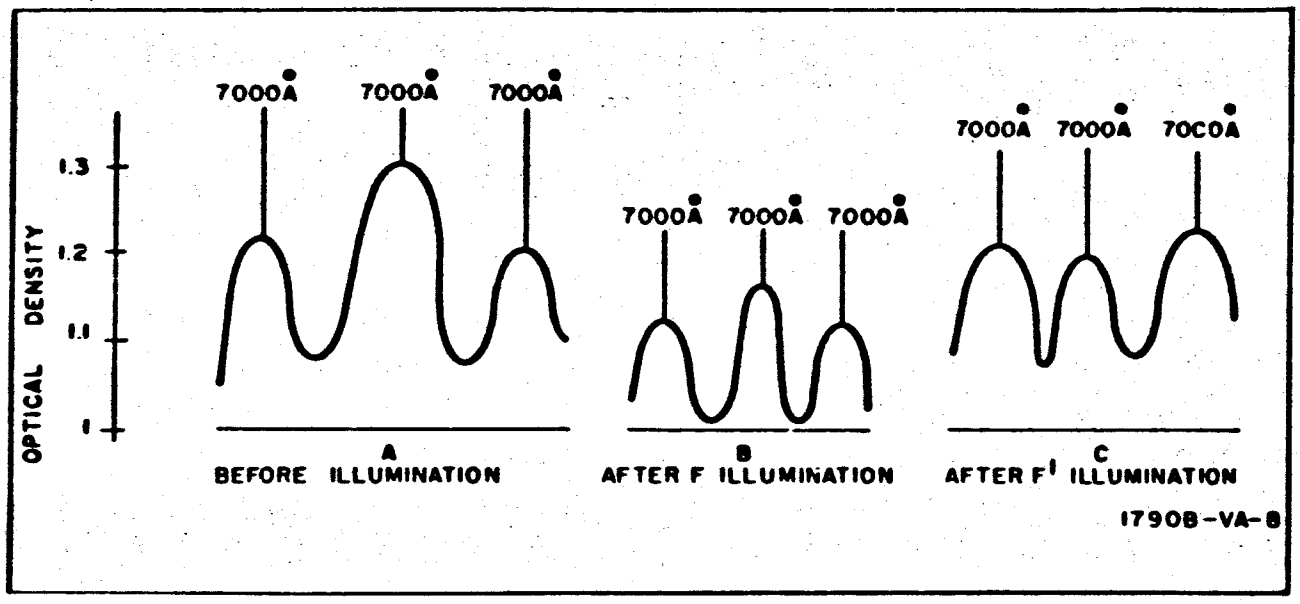

Figure 13. Illustration of Modulation Using The Carey Spectrophotometer

4. MERCURY CELL EXPERIMENT

4.1 EXPERIMENTAL SETUP

The mercury absorption cell itself was made of quartz tubing enclosed at the ends by two quartz flats. Attached to this cell by means of graded seals was a system of glass tubing leading to a Cenco vacuum pump, a superdry nitrogen supply, and a U-tube manometer filled with diffusion pump oil. The glassware was mounted on an optical bench in such a way that the axis of the quartz cell was parallel to the 4047 Å beam. Provision was made for moving the absorption cell in and out of the 4047 Å beam by means of a micrometer adjustment. The mercury used in the absorption cell and the two mercury lamps was natural mercury, since it was decided that any possible improvement in the experimental results as a result of using a pure isotope of mercury would not justify the expense.

The 4047 Å source was an electrodeless mercury-discharge tube driven by a 30-megacycle 30-watt oscillator coupled to the lamp by means of a coaxial cable. This lamp was blackened except for a narrow rectangular slit 3-mm high and 1.5-mm wide. Light from this slit was collimated by means of a 3-inch-focal-length f/3 lens. One 4047 Å interference filter was placed between the lamp and the absorption cell and another was placed in front of the 4047 Å photomultiplier. It was found that the first interference filter was not necessary, since removing it entirely did not affect the experiment in any way other than to increase the 4047 Å intensity. This result is reasonable in view of the fact that the collimating glass achromat blocked the 2537 Å line, the only line having sufficient power to alter the results appreciably.

The 2537 Å source was an electrodeless discharge lamp. It was made from 1/4-inch quartz tubing about 4 inches long and bent into the shape of an L. The short side of the L was 1-3/4 inches long and flattened so as to minimize self-reversal. In the experiment the long unflattened leg was eventually used because self-reversal effects were apparently quite small, and this leg could be

modulated more easily and uniformly. The lamp was driven by an Airborne Instruments Laboratory 10-watt oscillator through an isolator. It was modulated by a Hewlett Packard Model 200 C D 10 to 6 x 10^6 cps sine wave generator.

The 2537 Å lamp was placed so that one of its legs was parallel to the absorption cell. A condensing system consisting of two 3-inch diameter f/2 quartz lenses imaged this lamp onto the absorption cell, the length of the image being 1/4 inch high and very nearly equal to the length of the absorption cell. A Corning 7-54 filter in conjunction with a filter consisting of a solution of $NiSO_4 \cdot 6H_2O$ (concentration 240 grams per liter) and placed in a quartz cell 5 mm long and 1 inch in diameter isolated the 2537 Å line. DC measurements were made with two vacuum tube voltmeters and sine wave response measurements were made with an oscilloscope.

4.2 PROCEDURE

The mercury absorption cell and associated vacuum system was first outgassed thoroughly to eliminate any impurities. It should be emphasized here that the success of the experiment depended critically on the purity of the cell contents. Minute quantities of hydrogen in this system, for instance, strongly quenched the excited mercury atoms to ground rather than to the $6^3P/_o$ metastable state.

The first series of measurements were made by introducing small quantities of nitrogen into the absorption cell and measuring the steady-state induced absorption as a function of nitrogen pressure. First the system was evacuated to the mercury vapor pressure of the cell (1.2μ). Nitrogen was then added to bring the pressure up to about 100 mm of Hg, and the system was allowed to reach equilibrium. Then the system was slowly pumped out in steps of a few millimeters each, and a measurement was taken after each step. During this time both lamps were kept at constant brightness, and the 2537 Å source was shut off by inserting a piece of black cardboard into the path of the beam. Measurements were taken with the cardboard in and out of the path of the 2537 Å beam. Several runs were made in this manner and

the results recorded. The nitrogen pressure was read on a U-tube manometer containing Dow Corning 704 diffusion pump oil having a density of 1.07 grams per cc.

4.2.1 I_{4047} versus I_{2537}

It was noted that maximum absorption was induced at nitrogen pressures between 10 and 20 mm of Hg, so for this series of measurements the system was, as before, flushed with superdry nitrogen and then evacuated to a pressure of about 20 mm of Hg. This pressure remained the same throughout each of these runs. In each of these runs the brightness of the 2537 Å lamp was varied, and the 4047 Å induced absorption was measured at each brightness, both with and without the 2537 Å source blocked by the cardboard.

Since the 2537 Å lamp was imaged along the length of the absorption cell, it was necessary to take some precaution so that the brightness of the 2537 Å lamp would not vary along the length of the lamp. A very uniform brightness was achieved by carefully coupling the microwave osciilator to the 2537 Å lamp.

The 2537 Å lamp was monitored in two separate ways: by measuring the direct brightness at the rear of the lamp, and also by imaging the lamp onto an auxilary absorption cell by means of a quartz lens and measuring the intensity of the scattered 2537 Å light. Voltage readings were made with a voltmeter across the 10-kilohm photomultiplier tube load.

4.2.2 Sine Wave Response Measurements

In making sine wave response measurements an oscilloscope was used. The first problem was to determine how well the 2537 Å lamp itself followed a sine wave. Several runs were made on this lamp, directly monitored, in which the variation of the 2537 Å lamp was noted as the frequency of the driver was increased up to a maximum frequency of 600 kc. The lamp followed the driver without visible harmonic distortion except for a 3-db rise between 30 and 110 kc (figure 14). The detector was a photodiode in one case and a phototube in another, and the bandwidth of the circuitry for both exceeded the range of frequencies of the measurements. After these preliminary measurements, 4047 Å absorption variation was noted as the frequency of the 2537 A lamp

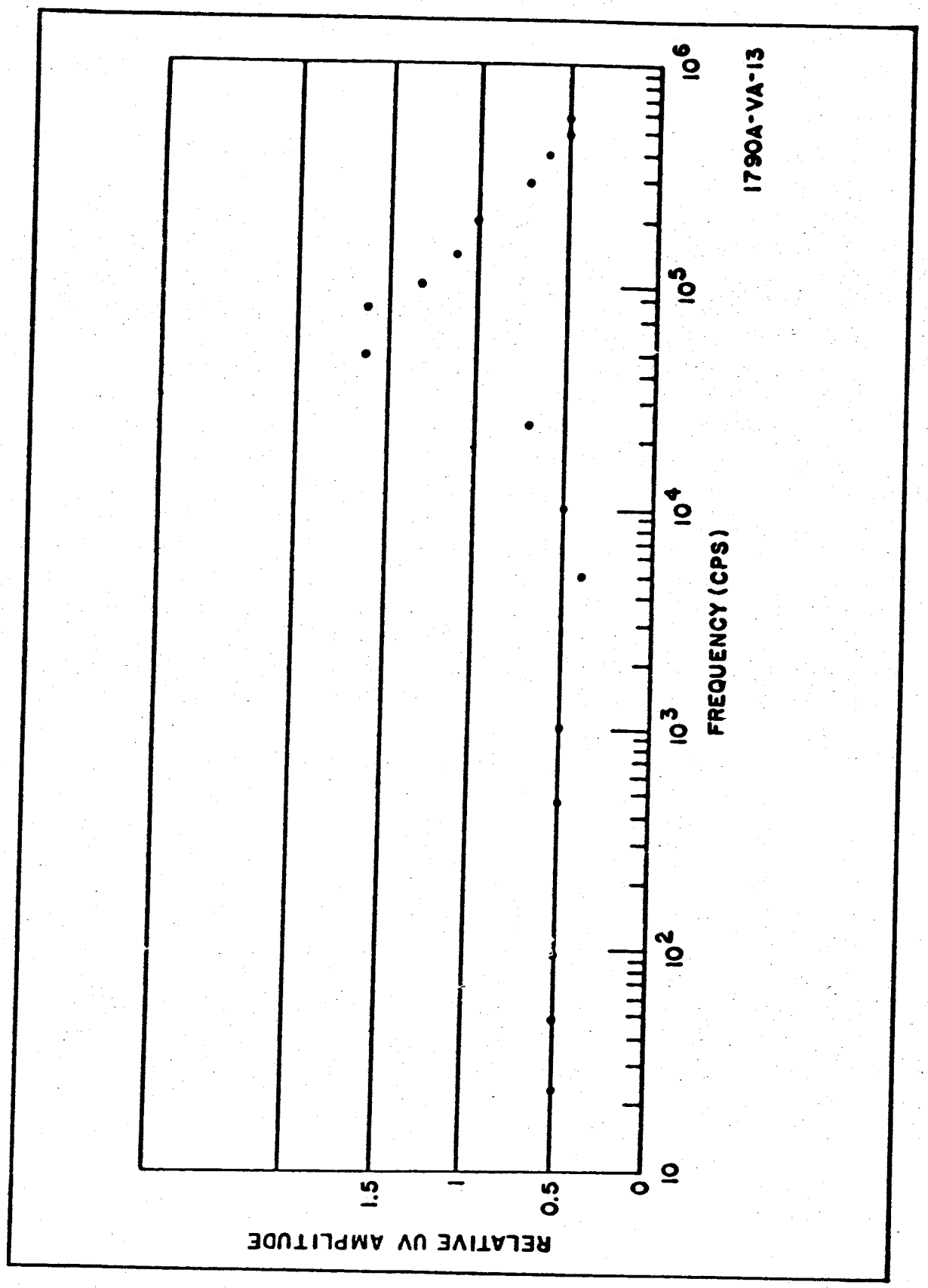

Figure 14. Frequency Response of the 2537 Å Lamp

output was varied. These runs were made with nitrogen pressure at about 20 mm of mercury.

4.3 EXPERIMENTAL RESULTS

4.3.1 Equilibrium Conditions

The percent of induced absorption depended on nitrogen pressure, 2537 Å intensity, spectral width of both lines, normal distance of the 4047 Å beam from the plane of incidence of the 2537 Å beam, and the length of the absorption cell, since the cell was run at constant (room) temperature. For low nitrogen pressures on the order of 1 to 4 mm of Hg there was a very small change in absorption as the beam was moved further away from 2537 Å incident; however, induced absorption was also small. With increased nitrogen pressure (4 to 30 mm of Hg) there was a tendency for the metastable energy levels to be confined nearer to the 2537 Å incidence, although this effect was not marked. For these pressure regions a notably higher induced absorption occurred. Finally, at high nitrogen pressures (50 mm of Hg) there was a marked and increasing tendency for the metastable energy levels to be confined near the 2537 Å incidence. At these pressures induced absorption fell off sharply. Figure 15 indicates, as noted above, that maximum absorption of about 50 percent occurred between nitrogen pressures of 10 and 20 mm of Hg.

The 4047 Å absorption as a function of 2537 Å intensity yielded two sets of results depending on the method of monitoring. Figure 16 shows the result of monitoring the 2537 Å radiation directly from the rear of the 2537 Å lamp. For small 2537 Å intensities, the intensity of the 4047 Å light decreased linearly with an increase of the 2537 Å intensity. As the intensity of the 2537 Å lamp was increased, by means of increasing the microwave power, the slope of the line I_{4047} versus I_{2537} decreased, indicating that either the 2537 Å line was broadening, or the dependence of the 4047 Å intensity no longer depended approximately linearly on the 2537 Å intensity. The 2537 Å intensity was then monitored by the scattering method mentioned above. Figure 17 is a plot of 4047 Å intensity versus 2537 Å intensity for the case in which the 2537 lamp was monitored by observing the intensity of 2537 Å radiation

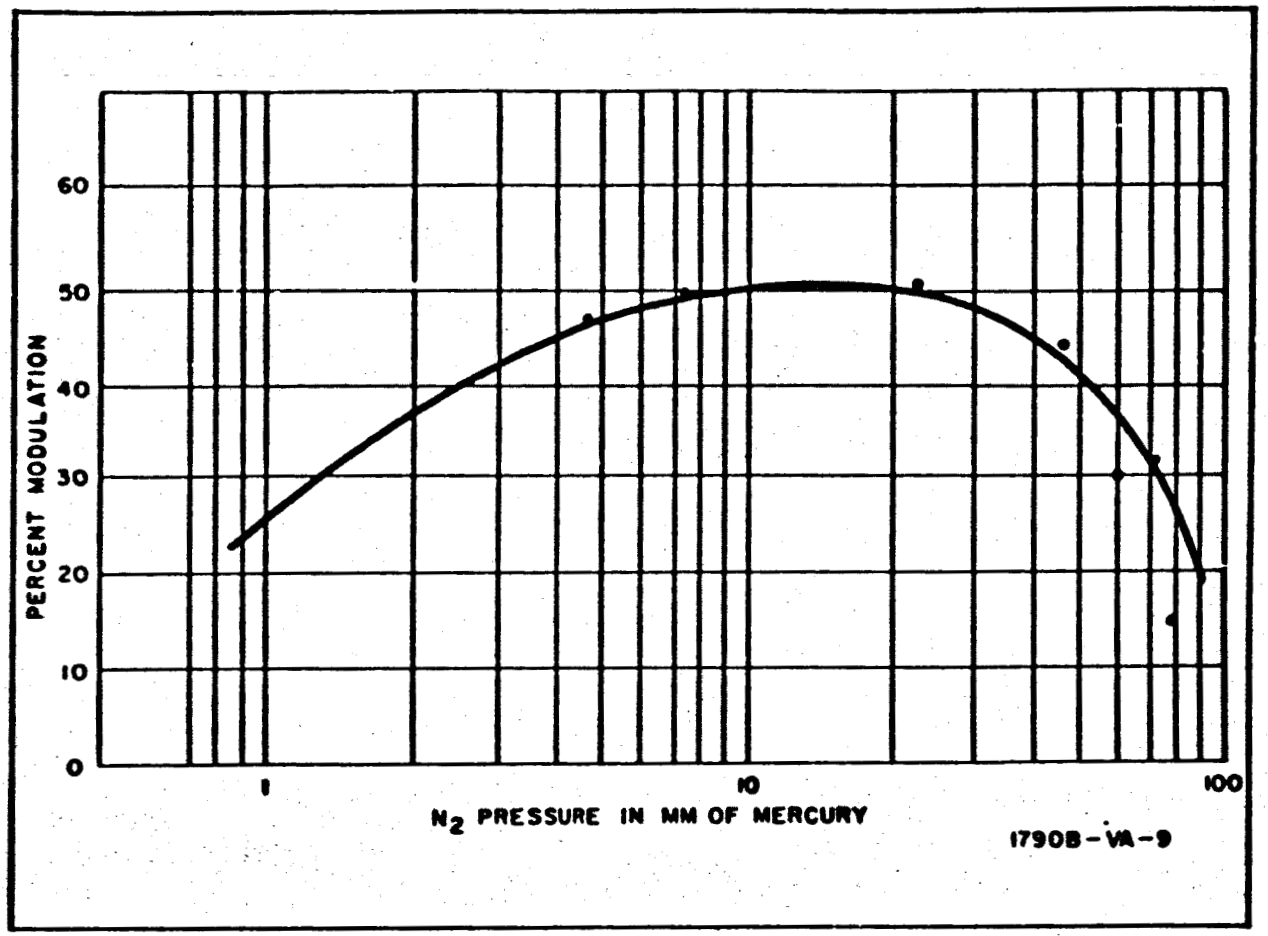

Figure 15. Percent Modulation of the 4047 Å Mercury Line as a Function of N_2 Pressure

scattered from a mercury absorption cell. This curve is seen to be very nearly linear.

4.3.2 Sine Wave Response

The sine wave response of the mercury cell modulation transfer element was found to remain reasonably flat to at least 10 kc for a nitrogen pressure of between 10 and 20 mm of Hg. Beyond this frequency, noise in the system predominated to such an extent that measurements could no longer be considered reliable. This noise was finally traced to the 4047 Å lamp and did not appear to diminish when another 4047 Å lamp was substituted.

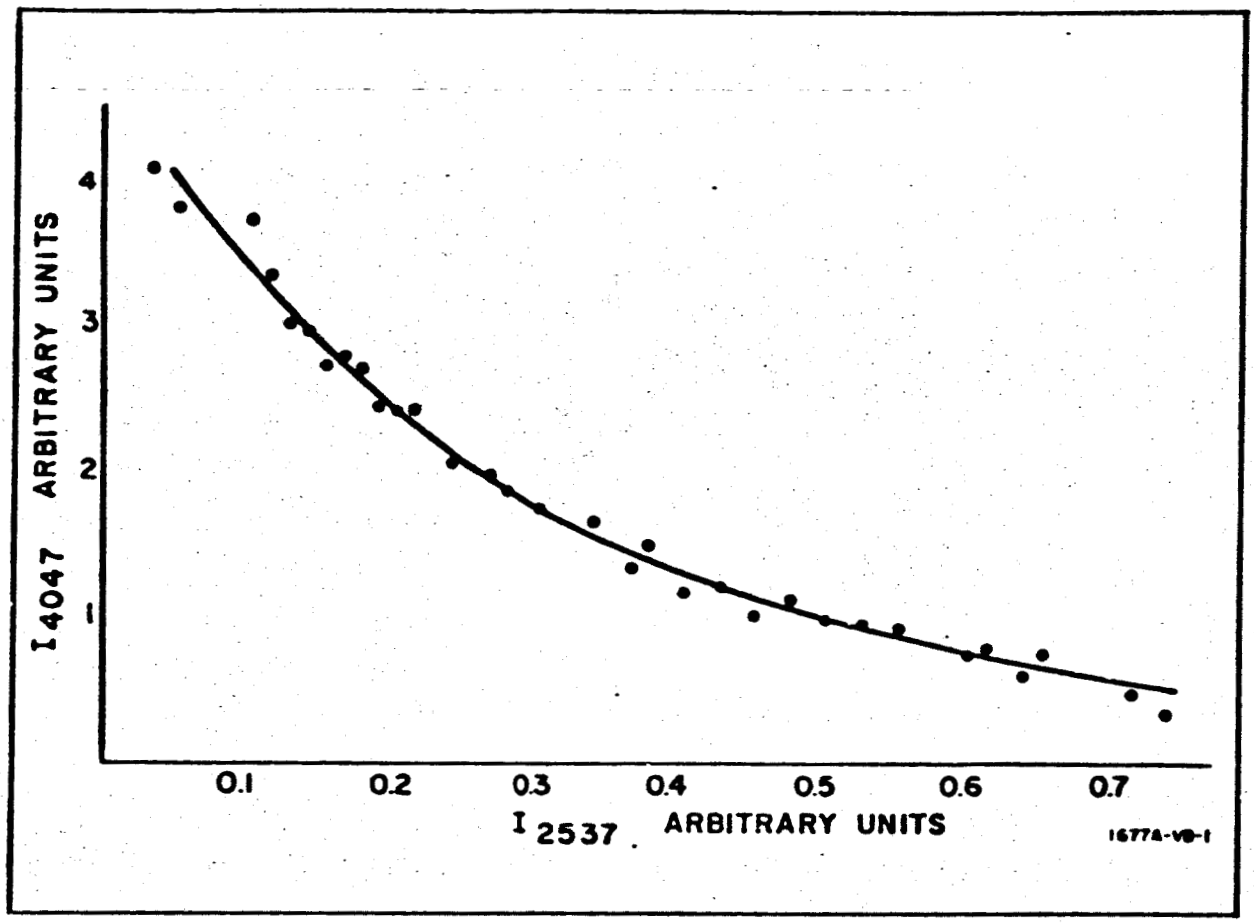

Figure 16. I_{4047} vs I_{2537}; I_{2537} Monitored Directly

4.3.3 Impurity Dependence

It was stated above that the experiment depended critically on impurities. The following brief discussion will elaborate on this dependence. The strong quenching abilities of impurities was noted very early in the experiment. When induced absorption could not at first be achieved; to locate the cause of the failure, several possibilities were investigated, one of which was the nitrogen supply. When the resonance radiation was scattered from the absorption cell, it was observed that adding nitrogen from the original supply to the cell quenched the scattered resonance radiation without causing absorption of the 4047 Å line. From these observations it was inferred that the 6^3P_o level never became appreciably populated. On this basis it was con-

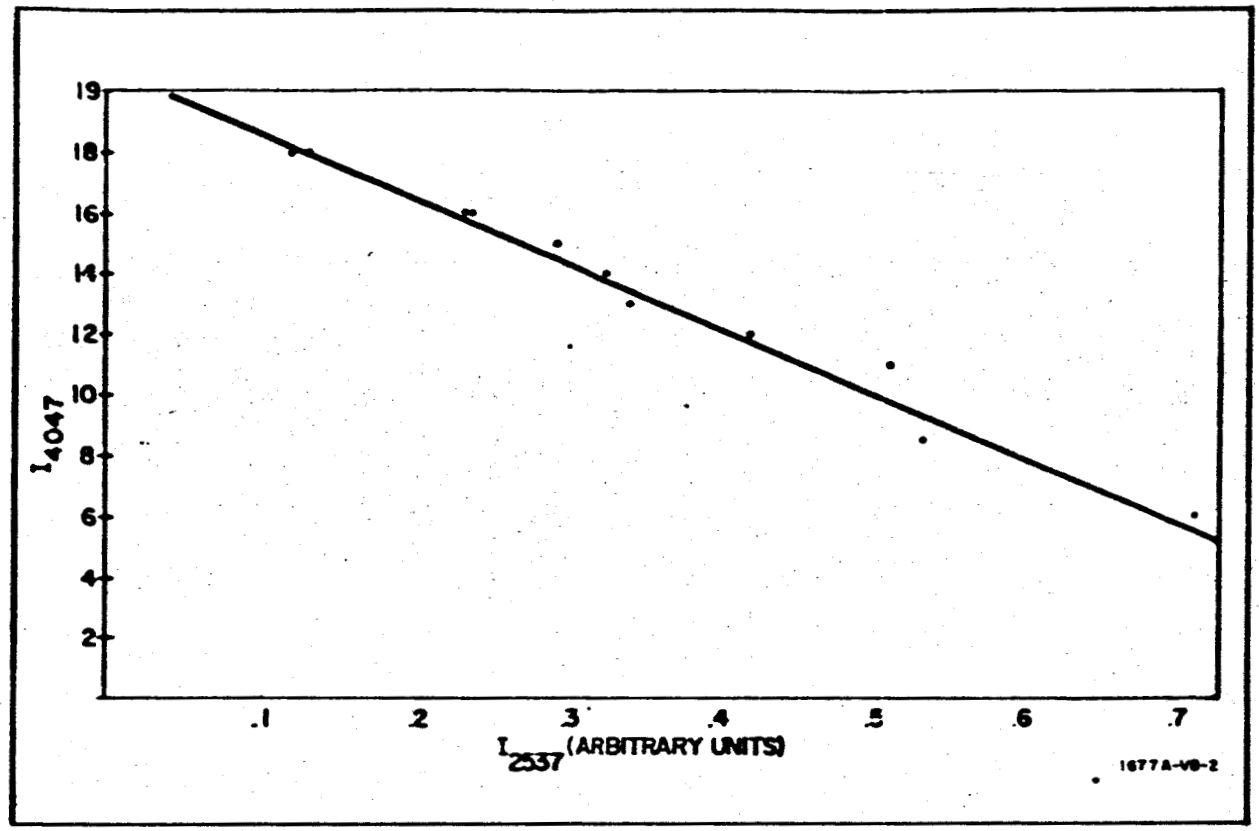

Figure 17. I_{4047} vs I_{2537}: I_{2537} Monitored by Scattering the Resonance Line From an Absorption Cell

cluded that the nitrogen supply contained enough impurities to reduce $6^3P_1 - 6^3P_0$ transitions drastically by producing an overwhelming number of $6^3P_1 - 6^1S_0$ transitions. The system was outgassed and flushed repeatedly with a fresh supply of superdry nitrogen. It was then possible to produce absorption of the 4047 Å line. Later in the experiment, the system was outgassed so well that a single supply of superdry nitrogen would produce the same measurable results for periods extending over several hours.

4.4 THEORY OF THE MERCURY CELL

4.4.1 Mathematical Formulation

An inspection of the mercury energy level diagram of figure 18 will show that there are five main energy levels to be considered in this experiment, 6^1S_o, 6^3P_2, 6^3P_1, 6^3P_o and 7^3S_o. Rate equations governing transitions to and from these levels together with two additional equations for absorption of the two beams constitutes a set of seven partial differential equations. This set, however, can easily be reduced to five because the intensities of the two beams are expressed in terms of the other unknowns. This set can be greatly simplified without unduly affecting the results if the following observations are noted.

It is well known that the absorption coefficient can be written in terms of the upper and lower states by the relation

$$\int_o^\infty k\,d\nu = \frac{\lambda_o^2}{8\pi} \frac{g_2}{g_1} \frac{n_1}{\tau}\left(1 - \frac{g_1}{g_2} \frac{n_1}{n_2}\right), \tag{13}$$

where

λ_o = the wavelength

g_1 and g_2 = statistical weights of levels 1 and 2 respectively,

n_1 and n_2 = population densities of levels 1 and 2, and

τ = the mean natural lifetime for spontaneous transitions from level 2 to level 1.

Since g_2/g_1 is equal to three, the last factor in parentheses is a very small quantity (since $n_2 \ll n_1$). Therefore, equation 13 can be written as

$$\int_o^\infty k\,d\nu \approx \frac{\lambda_o^2}{8\pi} \frac{g_2}{g_1} \frac{n_1}{\tau} \tag{14}$$

At the low vapor pressures inside a mercury electrodless discharge lamp, broadening is determined primarily by the doppler effect except at the wings of the line where Lorentz broadening predominates. In this discussion, doppler broadening alone will be assumed to determine line shape.

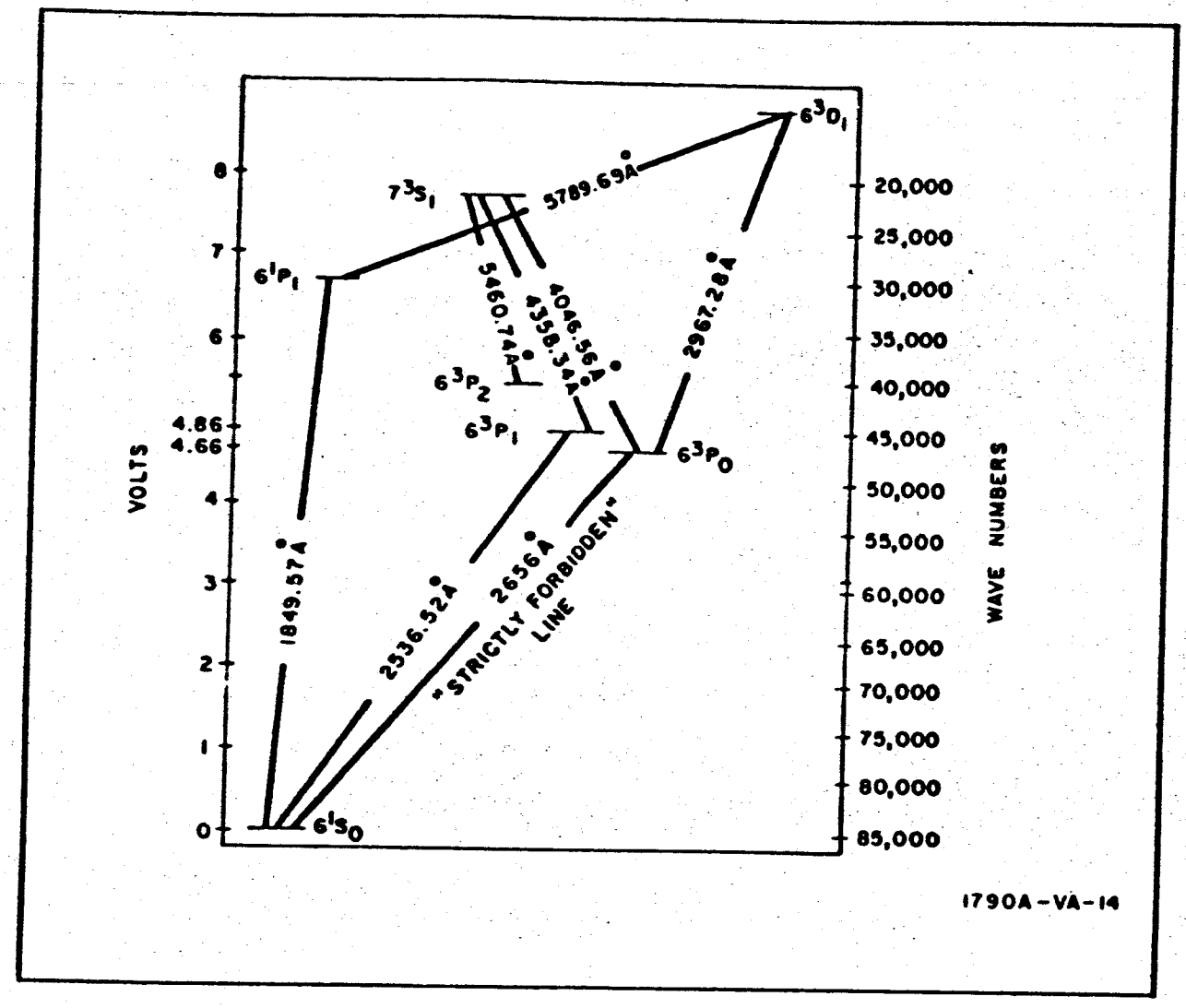

Figure 18. Energy Level Diagram of Mercury

In this case, equation 14 can be rewritten as:

$$\int k d\nu = \frac{1}{2}\sqrt{\frac{\pi}{\ell n_2}}\; k_o\, \Delta\nu_D = \frac{\lambda_o^2}{8\pi}\,\frac{g_2}{g_1}\,\frac{n_1}{\tau},$$

from which

$$k_o = \frac{1}{\Delta\nu_o}\sqrt{\frac{\ell n_2}{\pi}}\;\;\frac{\lambda_o^2}{4\pi}\;\frac{g_2}{g_1}\;\frac{n_1}{\tau} \qquad (15)$$

In addition to the above, the remaining simplifications will be made:

a. The ground state population will be considered constant; hence, the rate of population of the $^3P_1$ state due to absorption of the resonance line will

be kI, where k is the absorption coefficient in inverse centimeters, and I is the intensity of the 2537 Å line in photons/cm^2/sec.

b. Contributions of the 7^3S_1 energy level to the population density of either the 6^3P_1 or 6^3P_o states will be neglected.

c. Contributions from the $^3P_2$ level to the whole process will be neglected.

d. Diffusion effects will be neglected.

The first simplification is reasonable in view of the small amounts of power incident on the cell from the 2537 Å lamp. Under these illumination conditions, the ground state will always be so much more populated than any of the excited states that it can be thought of as a reservoir, whose small relative population changes are negligible.

The second simplification, while not as valid as the first in terms of relative population densities, nevertheless greatly eases the problem without altering the essential character of the results. Note that although the 7^3S_1 level can be populated in only one way, by upward transitions from the 6^3P_o level, it can be depopulated in three ways: by $7^3S_1 \rightarrow 6^3P_2$, $7^3S_1 \rightarrow 6^3P_1$, or $7^3S_1 \rightarrow 7^3S_o$ transitions; hence, only a fraction of the atoms leaving the 6^3P_o level because of 4047 Å absorption return to that level. Note also equation 14.

The third simplification is justified because of the small population densities of the 6^3P_2 level which would be produced under the weak illumination conditions of the present experiment. Since this level can only be populated by transitions from the 7^3S_1 level, any conclusions about small relative populations of that level would hold even more strongly for the 6^3P_2 level.

The fourth simplification is justified only on the grounds that it makes possible an uncomplicated solution which shows quite clearly and to a reasonable approximation the essential aspects of the problem. A rigorous solution should of course take into account diffusion processes.

After the above preliminaries, the basic equations will now be derived. Assume that one beam of light, the modulating beam, irradiates the absorption

cell uniformly along its length. In this experiment the modulating beam is at a right angle to the passive beam so the following equations are derived for this situation. Generalization to other situations are not difficult. Figure 19 illustrates the arrangement.

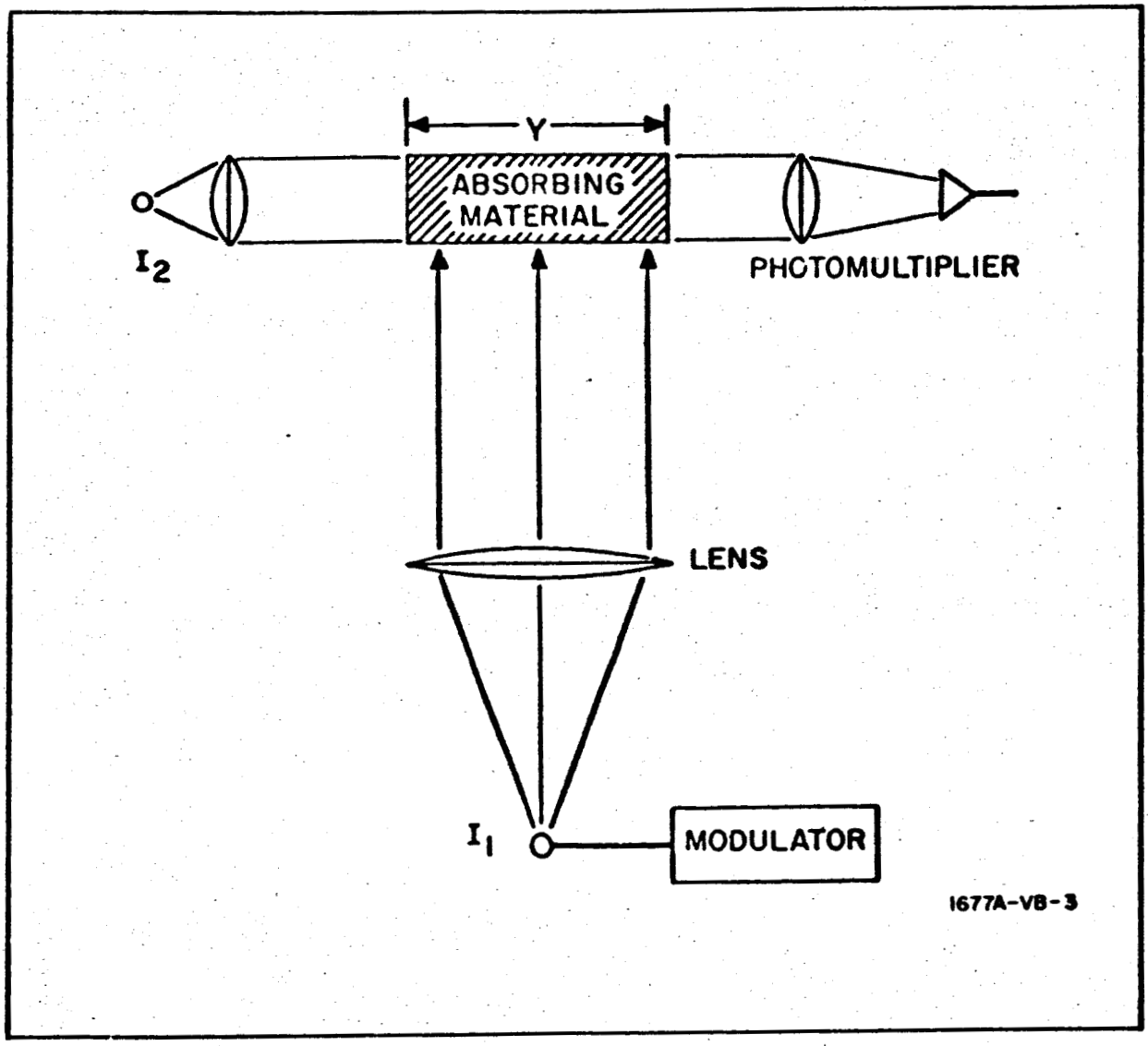

Figure 19. Arrangement Where Modulating Beam is at a Right Angle to the Passive Beam

The three equations describing the process are

$$\frac{\partial n_1}{\partial t} = kI_o e^{-kx} - a_{12} n_1 + a_{21} n_2 \qquad (16)$$

$$\frac{\partial n_2}{\partial t} = a_{12} n_1 - a_{21} n_2 - \frac{n_2}{\tau} - k' I' n_2 \qquad (17)$$

$$\frac{\partial I'}{\partial y} = - k' n_2 I' \qquad (18)$$

where,

n_1 = population density of the 6^3P_1 energy level,

n_2 = population density of the 6^3P_o energy level,

k = absorption coefficient in cm^{-1} for the 2537 Å line,

I_o = intensity in photons/cm^2-sec of the 2537 Å line,

a_{12} = rate per 6^3P_1 atom at which 6^3P_o atoms are created,

a_{21} = rate per 6^3P_o atom at which 6^3P_1 atoms are created,

τ = mean lifetime of the 6^3P_o energy level,

k' = absorption cross section in cm^2/atom for the 4047 Å line, and

I' = intensity of the 4047 Å line in terms of photons/cm^2-sec.

Equation 16 expresses the net rate at which the 6^3P_1 energy level is being populated. The first term on the right represents the rate at which atoms are arriving at this level due to 2537 Å line absorption. This term makes explicit use of the simplification that the ground state population is considered constant. Note that k, unlike k', contains the product of the absorption coefficient per atom/cc and the number of atoms/cc. Note also the exponential dependence on penetration depth.

Equation 17 expresses the net rate at which the metastable 6^3P_o atoms are created. The first two terms on the right represent the net rate at which collisions of the second kind of 6^3P_1 mercury atoms with N_2 molecules produce metastables. The third term on the right is the average lifetime of the metastable level. The fourth term expresses the rate of depopulation of the metastable due to 4047 Å line absorption. Here the population density appears explicitly as a dynamic factor in the induced absorption process.

Equation 18 expresses absorption of the 4047 Å line. Again, the explicit dependence on the population density of the metastable level is expressed.

If diffusion processes are included, terms of the form $D_i \nabla^2 n_i$ (i=1, 2), where

D_i = a diffusion coefficient and

∇^2 = the Laplacian operator, which should be added to the first two equations.

Although three equations are used to describe the induced absorption process, they can be reduced to two because of the relation 18. n_2 can be expressed in terms of I' through equation 18 in the following manner:

$$n_2 = -\frac{1}{k'I'} \frac{\partial I'}{\partial y} \tag{19}$$

$$= -\frac{1}{k'} \frac{\partial}{\partial y} \{\ell n\, I'\}$$

Equations 16 and 17 can now be written;

$$\frac{\partial n_1}{\partial t} = kIe^{-kx} - a_{12} n_1 - \frac{a_{21}}{k'} \frac{\partial}{\partial y} \{\ell n\, I'\} \tag{20}$$

$$-\frac{1}{k'} \frac{\partial}{\partial t} \frac{\partial}{\partial y} \{\ell n\, I'\} = a_{12} n_1 + \frac{a_{21}}{k'} \frac{\partial}{\partial y} \{\ell n\, I'\} + \frac{1}{k'\tau} \frac{\partial}{\partial y} \{\ell n\, I'\} + \frac{\partial I'}{\partial y} \tag{21}$$

4.4.2 Steady State Solution

Consider now the simplest case, the steady state solution. In this case the left sides of equations 20 and 21 vanish and the resulting pair of equations is easily solved:

$$kIe^{-kx} - a_{12} n_1 - \frac{a_{21}}{k'} \frac{\partial}{\partial y} \{\ell n\, I'\} = 0$$

$$a_{12} n_1 + \frac{a_{21}}{k'} \frac{\partial}{\partial y} \{\ell n\, I'\} + \frac{1}{k'\tau} \frac{\partial}{\partial y} \{\ell n\, I'\} + \frac{\partial I'}{\partial y} = 0$$

If the two equations are added, a single equation results;

$$kIe^{-kx} + \frac{1}{k'\tau} \frac{\partial}{\partial y} \{\ell n\, I'\} + \frac{\partial I'}{\partial y} = 0$$

This is easily integrated from y = 0 to y:

$$kIye^{-kx} + \frac{1}{k'\tau} \ell n(I'/I'_o) + I' - I'_o = 0 \tag{22}$$

I'_o is the intensity of the incident 4047 Å beam. Evidently, according to this approximation, if the lifetime is very long, I' becomes linearly dependent on I: for small modulations, the log term can be expanded about K_o'

$$kIye^{-kx} + \frac{1}{k'\tau}\left\{\frac{I_o' - I'}{I_o'} + \ldots\right\} + I' - I_o' = 0.$$

This can be written

$$I' = I_o'\left[1 - \frac{k'kIe^{-kx}y}{\frac{1}{\tau} + k'I_o'}\right] . \qquad (23)$$

Several facts are apparent from equation 23.

a. If $I_o' \to \infty$, $I' \to I_o'$; i.e., the ^3P_o level is pumped out too fast for any noticeable absorption to occur.

b. If $\tau \to 0$, $I' \to I_o'$. This shows why a metastable level is desirable.

c. I' varies linearly with y or I', i.e., doubling either y or I will have the same effect on I'.

d. I' varies exponentially with x, the distance from the face of incidence of the 2537 Å beam. Even considering diffusion, this will be generally true.

4.4.3 Effect of Spectral Distribution

Since spectral lines are not monochromatic, but are composed of distributions of wavelengths which vary under different physical conditions, some consideration must be given to the effect this variation will have on the results of the present experiment. Of particular interest in this section is the effect of the spectral variation of the 2537 Å line, since it is this line which will produce the modulation, and whose source will be subject to the widest physical variation since its brightness will be varied. One possible modulation scheme will be presented in which the spectral distribution of the 2537 Å source is modulated.

Theoretically, the effect of spectral variation of the 2537 Å line is contained in the first term in equation 22. This term should be replaced by an integration, i.e.,

$$kIye^{-kx} \rightarrow y \int_0^{\infty} k(\nu)\, I(\nu) e^{-k(\nu)x} d\nu \qquad (24)$$

Now it is not the purpose of this section to exhaust the implications of this integral. This has been thoroughly done by many theorists whose papers are readily available. It is in the interests of this section to consider the general effect of broadening and shifting the center of gravity of $I(\nu)$. For this purpose, two simple line shapes will be considered, a rectangular distribution and a Gaussian distribution.

In the case of a rectangular spectral distribution, the absorption coefficient will have a finite and constant value within a spectral range and will vanish outside this range. Likewise, the intensity of the source will have a constant value within a spectral range and will vanish outside this range; i.e.,

$$k(\nu) = k_o \quad \nu_o - \delta \leq \nu \leq \nu_o + \delta$$

$$= 0 \quad |\nu - \nu_o| > \delta$$

$$I = I_1 \quad \nu_o - \Delta \leq \nu \leq \nu_o + \Delta$$

$$= 0 \quad |\nu - \nu_o| > \Delta$$

where δ is the half width of the absorption line and Δ is the half width of the emission line.

In this case the integral of equation 24 becomes simply

$$2\delta k_o I_o y e^{-k_o x}, \quad \delta < \Delta, \text{ or} \qquad (25)$$

$$2 k_o \Delta I_o y e^{-k_o x} \quad \delta > \Delta \qquad (26)$$

If $\delta > \Delta$, that is, if the absorption line width is larger than the emission line width, any broadening of the emission will not affect the first term in equation 22 provided that the product $I_o \Delta$ (the integrated intensity of the emission line) remains constant. On the other hand, if $\delta < \Delta$, that is, if the

spectral width of the emission line exceeds that of the absorption line, the first term in equation 22 will be inversely proportional to the width of the emission line (assuming the constancy of the integrated intensity). To see this, examine the term 25 which is the one to use when $\delta < \Delta$. Since the product $I_1 = K$, $I_o = K/\Delta$, and 25 can be written

$$\frac{2\delta k_o K}{\Delta} y e^{-k_o x}.$$

This explains, in simple terms, the importance of preserving spectral width as the lamp brightness is increased, also the importance of monitoring the brightness of the 2537 Å lamp by the scattering technique mentioned in the experimental discussion.

For Gaussian line shapes, the integral becomes

$$y k_o I_o \int_0^\infty \exp\left[\frac{-(\nu-\nu_1)^2}{\delta^2} + \frac{-(\nu-\nu_1)^2}{\Delta^2}\right] \cdot \exp\left[-k_o x e^{-\frac{(\nu-\nu_1)^2}{\delta 2}}\right] d\nu \quad (27)$$

where

k_o = absorption coefficient at the line center ($\nu = \nu_1$).

I_o = intensity at $\nu = \nu_2$.

δ = to the absorption line width (width = $2\delta\sqrt{\ell n 2}$),

Δ = related to the emission line width (width = $2\Delta\sqrt{\ell n 2}$),

ν_1 = absorption line center and

ν_2 = emission line center.

The two spectral distributions have been centered at different frequencies for reasons which will presently be explained.

The integral, although rather complicated can be approximated by setting

$$\exp\left[-k_o x e^{-\frac{(\nu-\nu_1)^2}{\delta 2}}\right]$$

equal to

$$e^{-k_o x}.$$

Note that, while this term increases away from the line center, the first term in the integrand decreases rapidly, so that although the relative error of the approximated integrand can become large, the absolute value of the integrand is quite small. With this approximation equation 27 can be rewritten as

$$y k_o I_o e^{-k_o x} \int_o^\infty d\nu e^{-\left\{\frac{(\nu - \nu_1)^2}{\delta^2} + \frac{(\nu - \nu_2)^2}{\Delta^2}\right\}}$$

$$= \frac{\delta \Delta \sqrt{\pi}}{2\sqrt{\delta^2 + \Delta^2}} y k_o I_o e^{-k_o x} e^{-\frac{(\nu_1 - \nu_2)^2}{\delta^2 + \Delta^2}} \qquad (28)$$

Again the value of this term depends inversely on the emission line width, although this fact cannot be read directly from equation 8 as the condition of the constancy of the integrated intensity has not yet been imposed. This condition states that, for a Gaussian line,

$$\int_o^\infty I_o e^{-\frac{(\nu - \nu_2)^2}{\Delta^2}} d\nu = \frac{\Delta\sqrt{\pi}}{2} I_o = k.$$

Inserting this into 28 gives

$$\Theta = \frac{\delta k}{\sqrt{\delta^2 + \Delta^2}} k_o y e^{-k_o x} e^{-\frac{-(\nu_1 - \nu_2)^2}{\delta^2 + \Delta^2}} \qquad (29)$$

The inverse dependence of equation 29 on the emission line width is apparent. Note also that if $\delta >> \Delta$, equation 9 becomes essentially independent of either Δ or δ. If this term is put into equation 22, the result is

$$\frac{k k_o y \delta}{\sqrt{\delta^2 + \Delta^2}} e^{-k_o x} e^{-\frac{-(\nu_1 - \nu_2)^2}{\delta^2 + \Delta^2}} + \frac{1}{k'\tau} \ell n \left\{I'/I_o'\right\} + I' - I_o' = 0. \qquad (30)$$

The following observations can now be made:

a. As $\Delta \rightarrow \infty$ (k remaining constant), $I' \rightarrow I_o'$

b. As k_o, $x \rightarrow \infty$, $I' \rightarrow I_o'$

c. As k', $\tau \rightarrow \infty$, the equation becomes linearly dependent on K

d. If $\nu_1 - \nu_2 \rightarrow \infty$, $I' \rightarrow I_o'$.

The provision for ν_1 and ν_2 being in general unequal indicates that an induced modulation scheme can be devised in which ν_2 is varied with respect to ν_1. It also implies that it is not necessary to use the same element in both the gas cell and modulating lamp provided that a reasonable spectral match between the two can be made.

One scheme for modulating the 2537 Å lamp makes use of the Zeeman effect. On this case, ν_2 can be written as $\nu_1 \pm aH$, where a is a constant which depends on the energy levels involved in the emission line, and H is the magnetic field strength. In this case, $\nu_1 - \nu_2$ becomes $\pm$ aH, and equation 30 becomes

$$\frac{Kk_o y e^{-k_o x}}{\sqrt{\delta^2 + \Delta^2}} e^{-\frac{(aH)^2}{\delta^2 + \Delta^2}} + \frac{1}{k'\tau} \ell n \left\{ I'/I_o' \right\} + I' - I_o' = 0. \qquad (31)$$

Use of a magnetic field to modulate the 2537 Å source has only academic interest for steady state conditions and was introduced mainly as an exercise to illustrate the effects of spectral distribution on induced absorption.

4.4.4 Sinusoidal Modulation

A question of particular interest is the response of modulation transfer to a sinusoidal modulation of the 2537 Å lamp. For a solution to this problem reference is made to equations (20 and 21) which are repeated here for convenience.

$$\frac{\partial n_1}{\partial t} = kIe^{-kx} - a_{12}n_1 - \frac{a_{21}}{k'} \frac{\partial}{\partial y}\left\{\ln I'\right\}$$

$$-\frac{1}{k'}\frac{\partial}{\partial t}\frac{\partial}{\partial y}\left\{\ln I'\right\} = a_{12}n_1 + \frac{a_{21}}{k'}\frac{\partial}{\partial y}\left\{\ln I'\right\} + \frac{1}{k'\tau}\frac{\partial}{\partial y}\left\{\ln I'\right\} + \frac{\partial I'}{\partial y}$$

Let it be assumed that modulation is reasonably small. This allows the logarithm to be expanded around I_o'.

$$\ln I' = nI_o' + \frac{I' - I_o'}{I_o'} - \cdots\cdots \ln (I_o') - 1 + \frac{I'}{I_o'}$$

With this expansion, and noting that

$\frac{\partial}{\partial y}\left\{\ln I_o'\right\} - 1 = 0$, equations 20 and 21 become

$$\frac{\partial n_1}{\partial t} = k\,Ie^{-kx} - a_{12}n - \frac{a_{21}}{k'I_o'}\frac{\partial I'}{\partial y} \tag{32}$$

$$-\frac{I}{k'I_o'}\frac{\partial^2 I'}{\partial t\,\partial y} = a_{12}n_1 + \frac{a_{21}}{k'I_o'}\frac{\partial I'}{\partial y} + \frac{1}{k'\tau I_o'}\frac{\partial I'}{\partial y}\frac{\partial I'}{\partial y} \tag{33}$$

These equations can be solved for I' in terms of I by eliminating n_1 and reducing the set to a single equation. The algebra is tedious, so only the result will be given:

$$\frac{\partial}{\partial y}\frac{\partial^2 I'}{\partial t^2} + a\frac{\partial}{\partial y}\frac{\partial I'}{\partial t} + b\frac{\partial}{\partial y}I' = a_{12}k'I_o'\Theta \tag{34}$$

where:

$$a = a_{12} + a_{21} + \frac{1}{\tau} + k'I_o',$$

$$b = \left[\frac{1}{\tau} + k'I_o'\right] a_{12} \quad \text{and}$$

Θ = equation 29

The sine wave-response of (34) will be defined in terms of the amplitude of the ac component of I' in response to the ac component of Θ. Although the ac component will assume negative values, I and I' will, of course, never be negative. Hence Θ will be understood as following the variation described by $\frac{\Theta}{2}\left[1 + \cos \omega t\right]$. By considering only the ac component, the bias term is neglected. This, of course, does not alter anything essential.

The solution to the ac part of (34) is

$$I'_{ac} = \frac{-yk'I_o' a_{12}\Theta}{2\sqrt{(b-\omega^2)^2 + (a\omega)^2}} \cos(\omega - x). \tag{35}$$

$$\tan x = \frac{a\omega}{b\omega^2} \tag{36}$$

Evidently the amplitude of the ac component will remain fairly flat out to frequencies determined by $a\omega \approx b$, after which the falloff is essentially linear with ω. An estimate of this frequency can be obtained for typical values of the parameters in a and b for the present experiment:

$a_{12} \approx 10^6 \ \text{sec}^{-1}$

$a_{21} \approx 10^5 \ \text{sec}^{-1}$

$k'I_o' \approx 1 \ \text{sec}^{-1}$

$\tau \approx 10^{-3}$ sec, therefore

$a \approx 10^6 + 10^5 + 10^3 + 1 \sim 10^6$

$b \approx (10^3 + 1)\ 10^6 \approx 10^9.$

Therefore, the frequency response should remain fairly flat (in the present experiment) out to a frequency of the order of 1 kilocycle/sec. This somewhat pessimistic figure results from a conservative estimate of τ. Better results have actually been observed. It appears that the frequency response increases as lifetime decreases. Note however, that as $\tau \to 0$ $I_{ac} \to 0$. It is also of interest to note that, for low values of I_o' the frequency response increases linearly with the 4047 Å light level. This increase continues until $k' I_o'$ approaches $\frac{1}{\tau}$ after which there is a falloff from linearity. This is

reasonable, since an increase in I_o' should increase the rate of depopulation of the metastable level, resulting in an increased frequency response.

The parameter b can be associated with a "natural frequency" of the system. It will be shown in the next section, however, that there are no natural frequencies; i.e., the system cannot oscillate, at least to the approximations considered in this paper.

4.4.5 Step Function Response

If equation (34) is solved for the case of a step function in Θ ; i.e., $\Theta = 0$, $t < 0$, and $\Theta = \Theta_o$ $t > 0$ according to the initial conditions that $I' = \frac{\partial I'}{\partial t} = 0$, and the boundary condition that $I' = I_o'$ at $y = 0$, the solution is:

$$I' = I_o' \left[1 - \frac{k'y\ \Theta}{\left[\frac{1}{\tau} + k'I_o' \right]} \right] - \frac{yk'I_o'\, a_{12}\Theta}{S_1 - S_2} \left[\frac{e^{S_1 t}}{S_1} - \frac{e^{S_2 t}}{S_2} \right], \qquad (37)$$

where:

$$S_1 = -\frac{a}{2} + \frac{1}{2} \sqrt{a^2 - 4b}$$

$$S_2 = -\frac{a}{2} - \frac{1}{2} \sqrt{a^2 - 4b}$$

The term in S_1 and S_2 of interest is the radical because oscillation may or may not occur depending on whether the radical is imaginary, which would be the case if $a^2 - 4b < 0$. Oscillations are not possible however, as shown by the following consideration:

$$a^2 = (a_{12} + a_{21} + \frac{1}{\tau} + k'I_o')^2 > (a_{12} + \frac{1}{\tau} + k'I_o')^2$$

since $a_{21} \geq 0$,

Also, $4b = 4a_{12} \left[\frac{1}{\tau} + k'I_o' \right]$.

Therefore

$$(a_{12} + a_{21} + \frac{1}{\tau} + k'I_o')^2 - 4a_{12} \left[\frac{1}{\tau} + k'I_o' \right] > (a_{12} + \frac{1}{\tau} + k'I_o')^2$$

$$-4a_{12} \left[\frac{1}{\tau} + k'I_o' \right] = (a_{12} - \frac{1}{\tau} - k'I_o')^2 \geq 0$$

Therefore, $a^2 - 4b > 0$ and no oscillations can occur. Another question of interest is why the steady state ($t \to \infty$) condition does not contain either a_{12} or a_{21}. This appears to imply that the same induced absorption will occur whether $a_{12} = 0$ or . While the explanation is intuitive and similar to every other solution of this general form, it might be worthwhile to examine what happens when $a_{12} \to 0$. In this case

$$a \to a_{21} + \frac{1}{\tau} + k'I_o' \quad \text{and}$$

$$b \to 0, \text{ while}$$

$$S_1 \to 0 \text{ and } S_2 \to -a.$$

It is shown that the last term on the right in equation 37 vanishes, while the term containing $e^{S_1 t}/S_1$ is open to question because of the vanishing of S_1. Keeping this in mind, (37) can be rewritten, without the term containing $e^{S_2 t}/S_2$, in a rearranged form which is more useful;

$$I' = I_o' e^{-k'I_o' y \Theta_o} \left[\frac{1}{\frac{1}{\tau} + k'I_o'} + \frac{a_{12}}{S_1 - S_2} \frac{e^{S_1 t}}{S_1} \right] \qquad (38)$$

Since $S_1 \to 0$, the exponential term can be expanded around $S_1 = 0$; also remembering the definition of b, (21) becomes

$$I' = I_o' - k'I_o' y \Theta_o \left[\frac{a_{12}}{b} - \frac{a_{12}}{S_2} \frac{1}{S_1} - \frac{a_{12} t}{S_2} - \cdots \right] .$$

but $S_1 S_2 = b = a_{12} \left[\frac{1}{\tau} + k'I_o' \right]$, hence

$$I' = I_o' - \frac{k'I_o' y \Theta_o a_{12} t}{a_{21} + \frac{1}{\tau} + k'I_o'} \qquad (39)$$

This expression shows that no detectable absorption can be observed in any definite time as $a_{12} \to 0$ and implies that, though the final equilibrium conditions do not depend on a_{12} or a_{21}, the time to reach equilibrium most certainly does depend on these parameters. This fact could have been observed directly by noting that the first exponential term, S_1 0, hence the time constant, $\frac{1}{S_1} \to \infty$

as $a_{12} \rightarrow 0$, but the questions of the singularity and what to do with the second exponential term deserved to be resloved more completely.

4. 4. 6 Final Remarks on Spectral Distribution

Some concluding remarks on the effect of spectral distribution should be made at this time, since a discussion of the effect of spectral distributions of the 4047 Å emission and absorption lines has so far been neglected. In the present experiment this neglect is reasonable since the physical conditions of the 4047 Å lamp and absorption cell remained essentially unaltered throughout the experiment, thereby permitting the assumption that spectral distributions of the 4047 Å emission and absorption lines were constant parameters.

It is possible however, to imagine a general arrangement in which both lines might have variable width. In fact, it is possible that the emission and absorption lines might not even belong to the same element. For instance, the 4047 Å line might have been obtained with a tungsten lamp and monochrometer spelling arrangement. A similar situation might arise with the mercury 5461 Å line and iodine vapor where a close spectral match is well known to occur.

To see the effects of spectral distribution on the modulated line it is necessary to remember that equations (23), (35), and (37) actually pertain only to a small spectral region of the modulated light.

Examine equation (23);

$$I' = I_o' - \frac{yk'I_o' \, kIe^{-kx}}{\frac{1}{\tau} + k'I_o'}.$$

Note that the second term on the right contains the product $k'I_o'$. Suppose that the spectral width of k' is much less than that of I_o'. Then

$$ykIe^{-kx} \int \frac{I_o(\nu)\, k}{\frac{1}{\tau} + k'I_o'(\nu)} \, d\nu \; . \; < ykIe^{-kx} \int \frac{I_o(\nu)\, k'}{\frac{1}{\tau}} \, d\nu \; . \; << \int I_o' \, d\nu.$$

Hence $I(\nu)\, d\nu \sim I_o'(\nu)\, d\nu$, if the spectral width of the absorption line is much less than that of I_o', and modulation is consequently very small. Similar conclusions follow if the center of gravity of the spectral distribution of k' and I_o' are widely separated. Evidently, the effects are similar to those in the 2537 Å case discussed above, therefore mathematical arguments and conclusions concerning spectral distributions of the modulated line in equations (23), (35), and (37) will closely follow those for the 2537 Å emission and absorption lines. The details in any particular case can easily be worked out.

4.4.7 Evaluation of Parameters

In determining actual values of the parameters, k, k', a_{12}, a_{21}, and τ, recourse can be had both to theoretical and experimental results. Fortunately, much experimental data on the mercury spectrum is available, and where it is lacking, theory gives reasonable accuracy.

4.4.7.1 Absorption Coefficients

A theoretical expression for k_o (or k_o') was stated earlier (equation 3) for doppler lines. This expression can be written either in terms of the spontaneous emission probability or in terms of the f-number for the transition, thus

$$\frac{k_o}{N} = \frac{2}{\Delta\nu_D}\sqrt{\frac{\ell n 2}{\pi}}\ \frac{\lambda_o g_2}{8\pi g_1 \tau}$$

$$= \frac{2}{\Delta\nu_D}\sqrt{\frac{\ell n 2}{\pi}}\ \frac{\pi e^2}{mc} f$$

Experimentally, k_o/N, the absorption cross section for the 2537 Å line at the line center, as measured by Kopferman, yielded a value of 1.34×10^{-13} N cm^{-1}, by Kunge, 1.38×10^{-13} N cm^{-1}, and by Zemansky, 1.41×10^{-13} N cm^{-1}. Other experiments give similar values, so these values are apparently quite reasonable. Straight calculation from the formulas gives fair agreement with these values. Similarly, k_o', the absorption cross section at the 4047 Å line center, has been taken as 2.2×10^{-13} cm^2.

The distinction between absorption cross section and absorption coefficient should be kept in mind, namely that the absorption coefficient equals the product of absorbing centers per cc and absorption cross section. In the above theoretical development, k_o represents the absorption coefficient at the 2537 Å line center, while k_o' represents the absorption cross section at the 4047 Å line center. The two different definitions were a result of an assumption of constant density of ground state mercury atoms. The number of atoms per cubic centimeter is easily calculated, knowing the vapor pressure of mercury, from Loschmidt's number and the perfect gas law;

$$N = 2.685 \times 10^{19} \frac{273}{T} \frac{P}{760}, \text{ where}$$

T is the absolute temperature (~293° K) and P is the vapor pressure in millimeters of mercury. The vapor pressure of mercury at 293° K (20°C) is very nearly 0.0012 mm Hg, which makes

$$N = 2.69 \times \frac{273}{293} \times \frac{1.2}{760} \times 10^{16} = 3.96 \times 10^{13} \text{ atoms/cc}$$

This makes k_o, the 2537 Å absorption coefficient at the line center, nearly equal to $1.38 \times 10^{-13} \times 3.96 \times 10^{13}$ cm^{-1} = 5.45 cm^{-1}.

4.4.7.2 Collision Cross Sections

For these quantities, reference is made to an excellent paper by E.W. Samson. In this paper, collision cross sections for the $^3P_1 \rightarrow {}^3P_0$ transitions and $^3P_0 \rightarrow {}^3P_1$ were experimentally determined on the basis of the influence of nitrogen in increasing the fluorescene lifetime of mercury resonance radiation. His results are:

$^3P_1 \longrightarrow {}^3P_0$	$\sigma_{12}^2 = 3.1 \times 10^{-17}$ cm^2
$^3P_0 \longrightarrow {}^3P_1$	$\sigma_{21}^2 = 6.7 \times 10^{-18}$ cm^2
$^3P_1 \longrightarrow {}^1S_0$	$\Sigma_{10}^2 = 2.2 \times 10^{-18}$ cm^2
$^3P_0 \longrightarrow {}^1S_0$	$\Sigma_{20}^2 = 2.0 \times 10^{-22}$ cm^2 (roughly)

From these results it is a simple matter to calculate the collision probability per mercury atom per cc from the kinetic theory formula, namely

$$a_{ij} = 2N \sigma_{ij}^2 \sqrt{2\pi RT \left(\frac{1}{M_1} + \frac{1}{M_2}\right)} \left\{1 - \delta_{ij}\right\}, \; i, j = 1, 2$$

where a_{ij} is the number of collisions per second per mercury atom per cc for one of the four above collision transitions, N is the number of nitrogen atoms per cc, σ_{ij}^2 is the cross section, experimentally determined,

$R = 8.31 \times 10^7$ ergs/mole-deg,

T = absolute temperature, and

M_1 and M_2 are the molecular weights of nitrogen and mercury.

Again, taking T = 293° K, $M_1 = 14$, and $M_2 = 200$,

$a_{ij} = 7.08 \times 10^{21} \sigma_{ij}^2 p(1 - \delta_{ij})$, where p is the nitrogen pressure in mm Hg. If, for instance, p = 10 mm Hg,

$$a_{12} = 7.08 \times 10^{21} \times 3.1 \times 10^{-17} \times 10$$

$$= 2.2 \times 10^6 \frac{cc}{\text{sec-Hg atom}} .$$

4.4.7.3 Lifetime of the Metastable Atom

The term τ in the above equations includes not only the spontaneous decay lifetime of the metastable, but also any process other than the two explicitly defined in the rate equations. The most important decay process is diffusion to the cell walls where the metastables are reduced to ground upon collisions with the walls. Experimentally, it has been shown (M. L. Pool) that the natural lifetime of the metastable atom is at least 2.54×10^{-3} sec. since this was the maximum lifetime that could be produced by proper buffer gas pressure (5 mm Hg N_2 pressure). On the low pressure side of this maximum, the lifetime shortened quickly with decrease of N_2 pressure, indicating that the metastable mercury atoms were probably diffusing to the container walls and losing their energy unpon impact. On the high pressure side of the maximum, the decrease in metastable lifetime is due to the increasing number of collisions with nitrogen molecules. Figure 20 shows the lifetime of the metastable atom as a function of nitrogen pressure.

4.4.7.4 Possibility of Using the 4358 Å Line in Place of the 4047 Å Line

A question of interest in the present discussion is whether the 4358 Å mercury line could be used as the modulated line instead of the 4947 Å line. This line corresponds to the transition $7^3S_1 - 7^3P_1$, and since the 7^3P_1 level is the terminal level for 2537 Å absorption, would eliminate the intermediate collision process, $^3P_1 - {}^3P_0$ with its corresponding time

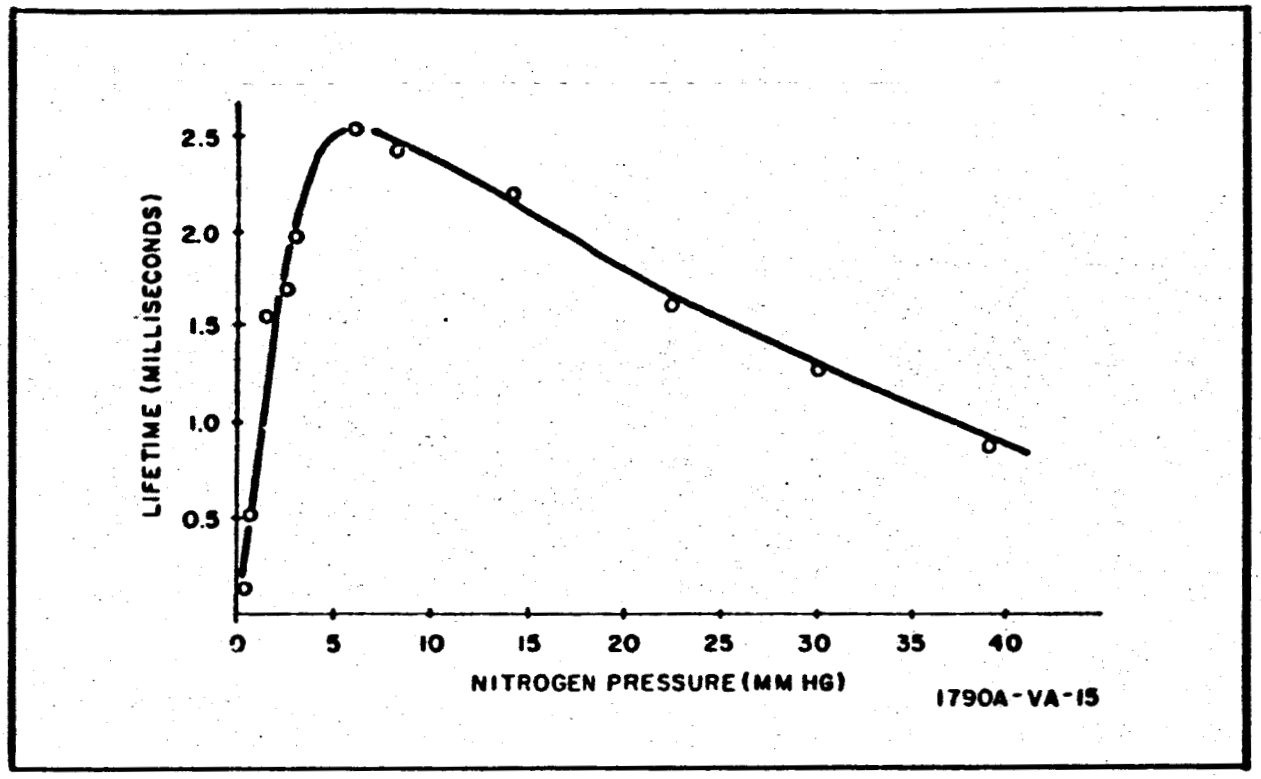

Figure 20. Lifetime of the Mercury Metastable as a Function of Nitrogen Pressure

constant. The chief advantage of using the 4047 Å line lies in the fact that the $^3P_0$ energy level is metastable and hence can be highly populated. Since there would be an advantage in frequency response to be gained by employing a direct transition, it might be worthwhile to add a brief discussion of this possibility.

At first thought it might be suspected that no appreciable modulation would be observed, since the $^3P_1$ state is populated for such a short time ($\sim 10^{-7}$ second).

However, some absorption of this line must occur, as is evidenced by the strength of the 5461 Å ($7^3S_1 - 7^3P_2$) line the emission of which is only possible if the 7^3S_1 state is achieved, and this can only be done by 4358 Å absorption. Experimental evidence that 5461 Å radiation occurs as a result of 2537 Å absorption followed by 4358 Å absorption is found in that the intensity

of the 5461 Å line in fluorescence is proportional to the square of the exciting radiation. Dr. E. Gaviola has shown theoretically that, when the intensity of the 4358 Å line is weak compared to that of the 2537 Å line, the number of atoms in the $^3P_1$ state at equilibrium is very nearly

$$n_{^3P_1} = k \tau_{^3P_1} I_{2537}$$

$$= k \tau_{^3P_1} I^o_{2537} e^{-kx}, \text{ where}$$

$n_{^3P_1}$ = number of atoms per cc in the 6^3P_1 state,

k = absorption coefficient for the 2537 Å line,

x = length of the absorption cell,

$\tau_{^3P_1}$ = average lifetime ($\approx 10^{-7}$ secs) of the 6^3P_1 state, and

I_{2537} = intensity of the 2537 Å line. On this basis, he derived an absorption law for the 4358 Å line given by

$$I_{4358} = I^o_{4358} e^{-k' \tau_{^3P_1} I_{2537} \left[1 - e^{-kx}\right]}$$

where k' is, again, the absorption cross section for the 4348 Å line, and the two beams are parallel. Assuming that $k' \sim 10^{-12}$, $\tau_{^3P_1} \sim 10^{-7}$, $k \sim 5$, and $x \sim 2$ cm.

$$I_{4358} = I^o_{4358} e^{-10^{-19}} I_{2537}.$$

Suppose that 1 milliwatt per cm^2 sec is incident on the face of the absorption cell. This will contain

$$\frac{\lambda \times 10^{-3}}{6.62 \times 10^{-34} \times c} = \frac{2.54 \times 10^{-8}}{6.62 \times 3 \times 10^{-24}} \text{ photons } cm^2\text{-sec} = 1.28 \times 10^{15}$$

photons/cm^2-sec. Therefore $I_{4358} = I^o_{4358} e^{-1.28 \times 10^{-4}}$ and absorption is evidently small.

Matters can be improved somewhat if the 4358 Å line and 2537 Å line are at right angles. In this case, at equilibrium

$$I_{4358} = I^{o}_{4358}\, e^{-k' k \tau_{3_{P_1}} I_{2537}\, y e^{-kx}}$$

The short lifetime can be partially offset by increasing the cell length, however, this of course requires additional power.

5. CONCLUSIONS

The advantages of the mercury cell modulation transfer element are that it is simple, highly reliable, and long lived, does not depend on polarization, and is almost insensitive to background radiation because of its narrow spectral region of response. It comes the closest to being an ideal MIROS element. Its chief disadvantage is its lack of any spectral versatility. The transmitter light must be 2537 Å and the receiver light must be 4047 Å. These wavelengths are very inconvenient from two standpoints. First, no adequate light source at these wavelengths is at present available and secondly, atmospheric transmission does not occur at 2537 Å.

Potassium iodide, because of its broad absorption bands, has the advantage of spectral versatility, enabling it to operate with some of the best available laser sources. Spectral selection could be accomplished with interference filters. Unfortunately, the frequency response of potassium iodide is very poor. Also, because of their sensitivity to light the crystals must be carefully prepared. This sensitivity could be a disadvantage because of possible light leaks which might severely limit the operating lifetime of these crystals. Therefore although potassium iodide, satisfies one of the requirements, it is in other respects at this stage of development far from being an ideal passive modulation transfer element.

What is now required is further research and development in order to produce a passive modulation transfer element which combines the advantages of mercury vapor and potassium iodide. If a substance similar to mercury vapor with its ultranarrow spectral response is to be developed to practicality, its absorption lines must coincide with spectral lines of the best available laser sources. A research program involving solid state materials such as potassium iodide would have as its purposes the improvement of frequency response and the production of more efficient and reliable

materials.

On the basis of both the experimental and theoretical results obtained during the MIROS program it can certainly be concluded that passive modulation transfer between two light beams is possible. It has been demonstrated not only that appreciable modulation can be achieved, but also that reasonable bandwidths are obtainable. In this sense the MIROS program can be considered to have been successful.

It is also possible at this time to define the characteristics of an ideal modulation transfer element in terms of transition probabilities, absorption coefficients, cross sections, and optical intensities. For instance, it is seen that, where a series of intermediate levels are involved, the time constants for the process increase and consequently the frequency response decreases. Therefore, in order to produce an efficient modulation transfer element, it is desirable to limit the number of intermediate transitions to as few as possible. The mercury cell required one intermediate transition, namely nitrogen-quenching collisions with excited mercury atoms. The theoretical discussion showed that the absorption time constants were essentially determined by this process.

The results of the MIROS program, therefore, are that passive optical modulation transfer has been demonstrated, and an expression has been developed which indicates the key items for maximizing the process efficiency. Also, an estimate of the power required in the ideal case has been given.

Although the MIROS program has been successful in that passive modulation transfer has been demonstrated, a practical system is not a present reality. Spectral response regions of these modulation transfer elements do not coincide with the spectral regions of the most desirable laser sources except in the case of solid state materials where the time constants are discouragingly long.

6. RECOMMENDATIONS

If a practical modulation transfer element is to be developed, spectral regions of laser sources must be matched. In order to achieve this matching, a systematic examination of elements and compounds must be undertaken, and a good deal of ingenuity will be needed to find combinations of transitions which would satisfy the requirements of a practical MIROS system. To begin with, the transmitter light must correspond to transitions from a ground or quasi-ground state. For most of the atomic elements these transitions correspond to short wavelengths. Some elements, especially those with doublet fine structure, offer the possibility of operating at microwave frequencies corresponding to hyperfine transitions, although even with this help a satisfactory match with useful laser sources has not been made. In addition many substances which might offer favorable spectral response will operate only at high temperatures, or their response times are not satisfactory.

Therefore, a MIROS program very similar to the research programs presently underway in the laser field is recommended. This program should include a study of presently known and potential methods of optical pumping. It would require a systematic investigation of molecular vibrational and rotational spectra as well as crystal and solid state absorption spectra.

7. NEW TECHNOLOGY

During this program two possibly new technologies have been developed. The basic concept behind the mercury cell experiment could lead to the development of efficient passive optical modulation transfer elements. The experiments performed on potassium iodide crystals are, to the best of our knowledge, new, in so far as no information on potassium iodide absorption bands was discovered after considerable search of the literature. Also, efficient passive optical modulation transfer devices, capable of reasonable information rates, could be the result of the potassium iodide experiments during the MIROS program. The details of these two experiments are covered in Section 3 and Section 4 of this report.

BIBLIOGRAPHY

BOOKS

Born, M., and E. Wolf, Principles of Optics, London: Pergammon Press, 1959.

Dekker, A. J., Solid State Physics, Englewood Cliffs, N. J.: Prentice-Hall, Inc., 1957.

Jeans, J., An Introduction to The Kinetic Theory of Gasses, Cambridge: Cambridge University Press, 1962.

Kittel, Charles, An Introduction to Solid State Physics, New York: John Wiley and Sons, Inc., 1956.

Mitchell, A., and M. Zemansky, Resonance Radiation and Excited Atoms, Cambridge: Cambridge University Press, 1961.

Moss, T. S., The Optical Properties of Semi-Conductors, London: Butterworth Press, 1961.

Mott, N. F., and R. W. Gurney, Electronic Processes in Ionic Crystals, Oxford: Clarendon Press, 1950.

Strong, J., Concepts of Classical Optics, San Francisco: Freeman Press, 1958.

PERIODICALS

Costikas, A., and L. S. Grossweiner, "Photoequilibrium Between KC1 F and F' Centers at 80°K," Physical Review, Vol. 126, No. 4 (May 15, 1962).

Goviola, E., "The Power Relation of the Intensities of the Lines in the Optical Excitation of Mercury." Philosophical Magazine, 6, 1154, 1167 (1926).

Kamshilina, U. M., "The Quenching of Mercury Resonance Radiation in a Gaseous Discharge," Optics and Spectroscopy, 14, 14 (April 1963).

Kleinschrod, F. G., Annal de Physik, 27, 97 (1936).

Markham, J. J., "Interaction of Normal Modes with Electron Traps," Review of Modern Physics, Vol. 31, No. 4 (October 1959).

Ottmer, R., Zeitschrift fur Physik, 46, 798 (1928).

Pohl, R. W., Proceedings of the Physical Society, 49, 3 (1937).

Pool, M. L., "Life of Metastable Mercury and Evidence for a Long-lived Metastable Vibrating Nitrogen Molecule," Physical Review, Vol. 38 (September 1931).

Samson, E. W., "Effects of Temperature and Nitrogen Pressure on the Afterglow of Mercury Resonance Radiation," Physical Review, Vol. 40 (June 1932).

Seitz, F., "Color Centers in Alkali Halide Crystals I," Reviews of Modern Physics, Vol. 18, No. 3 (July 1946).

Seitz, F., "Color Centers in Alkali Halide Crystals II," Reviews of Modern Physics, Vol. 26 (January 1954).

Zito, R., and A. E. Schraeder," Optical Excitation of Mercury Vapor for the Production of Isolated Fluorescence," Applied Optics, Vol. 2, No. 12 (December 1963).

REPORTS

Goodell, J., MIROS Monthly Report No. 7, Aerospace Division, Westinghouse Electric Corporation, December 1963.

APPENDIX I

Given a solid and a vapor in equilibruim, the free energy of the system $G = E - TS$ is conserved. Here G = Gibbs free energy, E = total energy, T = temperature and S = entropy of the system. The free energy of a monoatomic vapor containing n_v atoms/cm^3 is given by:

$$n_v kT \left[\log \left(\frac{2\pi\, mkT}{h^2} \right)^{3/2} + \log \left(\frac{1}{n_v} \right) + 1 \right]$$

where k = Boltzman's constant, h = Planck's constant, T = absolute temperature, m = mass, and n_v = number of atoms/units volume. Thus, if one atom is removed from the vapor the free energy increases by:

$$KT \left[\log \left(\frac{2\pi\, mk\, T}{2} \right)^{3/2} + \log \frac{1}{n} \right]$$

This free energy has to be balanced when adding one atom to the crystal as an F-center. Let the energy required to add one atom to the solid be designated as W_F and let the solid contain N ion pairs and n_F F-centers. Then its entropy is:

$$k \log \left(\frac{N + n_F !}{n - !N!} \right)$$

if the amount of dissociation is negligible. If now n_F is increased by one, and

$$k \log \frac{(N + n_1 = +1)!}{(n_F + 1)\ \ !N!}$$

is subtracted from the previous expression, the entropy change due to addition of an F-center is obtained as

$$k \log \frac{n_F + N}{n_F}.$$

The condition for equilibrium for balance of free energy then gives

$$W_F - k\,T \left[\log \frac{N + n_F}{n_F} + k\,T \log \frac{(2\pi\, m\, k\, T)^{3/2}}{h^2} + k\,T \log \frac{1}{h\nu} \right] = 0. \quad (5)$$

This expression can be written

$$\frac{n_F}{N + h_F} = n_v \left(\frac{2\pi\, m\, k\, T}{h^2}\right)^{3/2} = h_v \left(\frac{2\pi\, m\, k\, T}{h^2}\right)^{3/2} e^{-W_F/kT}$$

In this formula, the coefficient of the exponential is not reliable since the free energy due to vibrating atoms was neglected. Once m_F/m_v is known as a function of temperature, W_F is the activation energy for this process and can be obtained from the slope of the curve h_F/h_v versus $1/kT$. Plotting the experimental data it turns out that for KC and KBr W_F is -0.1 and -0.25 respectively. This given an approximate magnitude for W_F in alkali halides.

APPENDIX II

In estimating the crystal thickness necessary for 10 percent modulation for a specific number of absorbing centers/cm^3 the following exercise will be helpful. Consider Maxwell's equations with the usual meaning of symbols:

$$\nabla \times \vec{E} = - \mu\mu_o \frac{\partial H}{\partial t} \tag{1}$$

$$\nabla \times \vec{H} = \sigma \vec{E} + \epsilon\epsilon_o \frac{\partial E}{\partial t} \tag{2}$$

$$\nabla \vec{H} = 0 \tag{3}$$

$$\nabla \vec{E} = 0 \tag{4}$$

then

$$\nabla \times \nabla \times \vec{E} = -\mu\mu_o \left(\sigma \frac{\partial \vec{E}}{\partial t} + \epsilon\epsilon_o \frac{\partial^2 \vec{E}}{\partial t^2}\right).$$

using the first and second equations and interchanging the order of taking the curl with the time derivative on $\vec{H}$. Using the identity

$$\nabla \times \nabla \times \vec{E} = \nabla (\nabla \vec{E}) - \nabla^2 E \tag{5}$$

and the fourth equation, one obtains a wave equation of the form

$$\nabla^2 \vec{E} - \sigma \mu\mu_o \frac{\partial \vec{E}}{\partial t} - \mu\mu_o \epsilon_o \frac{\partial^2 \vec{E}}{\partial t^2} = 0 \tag{6}$$

of which a solution is the travelling wave

$$U_x = U_o e^{-(t - \frac{x}{v}) i\omega} \tag{7}$$

if

$$\frac{1}{v^2} = \mu\mu_o \epsilon\epsilon_o - \frac{i\sigma\mu\mu}{\omega}$$

V, in a material, is given by $\frac{n}{c}$ (n being the index of refraction). Hence,

$$n^2 = c^2 (\mu\epsilon - \frac{i\sigma\mu}{\omega\epsilon_o} \quad \mu_o \epsilon_o$$

Since

$$c^2 = \frac{1}{\mu_o \epsilon_o} ,$$

$$n^2 = \mu\epsilon - \frac{i\sigma\mu}{\omega\epsilon_o} \qquad (8)$$

This indicates a complex n of the form n = a - ik. U_x now becomes

$$U_o e^{i\omega t} e^{i\omega nx/c} e^{- \omega kx/c} \qquad (9)$$

(μ for nonmagnetic materials is 1).

The absorption coefficient of a medium, K is defined in such a way that the energy in the wave falls to $\frac{1}{e}$ of its value along a distance $\frac{1}{K}$. Since the Poynting's vector is proportional to the product of the electric and magnetic vectors, and, since both these terms contain $e^{- kx/c}$, the attenuation will be $e^{-2\omega kx/c}$. Along a travel distance of $\frac{1}{K}$ the exponent should drop to $\frac{1}{e}$ yielding $K = \frac{2\omega k}{c} = \frac{4\pi k}{\lambda}$. It is this K, which, for a certain doping and thickness of the crystal, is sought.

Let us suppose that a given impurity center gives rise to an absorption line with a breadth $\Delta\nu$ and an excitation coefficient B. Then the probability that one quantum will be absorbed is given by $IB/\Delta\nu$, where I is the radiation intensity in ergs/cm^3. If there are n quanta/sec and N absorbing centers/cm^3 then I becomes $h \cdot \nu \cdot n/c$, and the number of quanta absorbed/cm^3-sec is $IBN/\Delta\nu$. Putting $\pi e^2 f/h \cdot \nu \cdot m$ for B, 1/2 for f and 0.5 ev for h ν, k equals N x 10^{-16} cm^{-1}, relating the absorption coefficient and the number of absorbing centers for a certain value of $\Delta\nu$. The thickness of the crystal can now be estimated for a definite percent absorption, if the F-center concentration is known.